Mon. Not. R. Astron. Soc. **000**, 000–000 (2002)

The rms peculiar velocity of galaxy clusters for different cluster masses and radii

Ivan Suhhonenko and Mirt Gramann
Tartu Observatory, Tõravere 61602, Estonia

12 March 2002

ABSTRACT

We investigate the rms peculiar velocity of galaxy clusters in the Lambda cold dark matter (ΛCDM) and tau cold dark matter (τCDM) cosmological models using N-body simulations. Cluster velocities for different cluster masses and radii are examined. We analyze simulations carried out by the adaptive particle-particle/particle-mesh (AP^3M) and by the particle-mesh (PM) codes with the same mass resolution. To identify clusters in the simulations we use two methods: the standard friends-of-friends (FOF) method and the method, where the clusters are defined as the maxima of the density field smoothed on the scale $R \sim 1h^{-1}$ Mpc (DENSMAX). We find that in the AP^3M simulations, the rms velocity of clusters defined with the DENSMAX method is almost independent of the cluster density. The rms velocity of FOF clusters decreases with the cluster mass and radius. In the ΛCDM AP^3M model, the rms peculiar velocity of massive clusters with an intercluster separation $d_{cl} = 50h^{-1}$ Mpc is $\approx 15\%$ smaller than the rms velocity of the clusters with a separation $d_{cl} = 10h^{-1}$Mpc. Contrary, in the PM simulation, the rms peculiar velocity of massive clusters is higher than the rms velocity of low-mass clusters.

Key words: galaxies: clusters: general – cosmology: theory – dark matter – large-scale structure of Universe.

1 INTRODUCTION

One of the interesting unknowns in cosmology is the large-scale peculiar velocity field in the Universe. The peculiar velocity field can be studied by using galaxies or clusters of galaxies. However, there are some advantages in studying the peculiar velocity field by using galaxy clusters. One of these advantages comes from the fact that, on scales probed by galaxy clusters, the velocity fluctuations are largely in the quasi-linear regime and close to the initial state from which large scale structures developed. In addition, peculiar velocities of clusters can be determined more accurately than peculiar velocities of galaxies since the distance to each cluster can be obtained from a large number of member galaxies, thus considerably reducing the velocity uncertainties of clusters. Cluster motions could therefore provide an important tool in probing the large-scale peculiar velocity field.

Peculiar velocities of clusters of galaxies have been studied in several papers (e.g. Bahcall, Gramann & Cen 1994; Lauer & Postman 1994; Bahcall & Oh 1996; Moscardini et al. 1996; Borgani et al. 1997; Watkins 1997; Dale et al. 1999; Hudson et al. 1999; Borgani et al. 2000; Colless et al. 2001). Watkins (1997) developed a likelihood method for estimating the rms peculiar velocity of clusters from line-of sight velocity measurements. This method was applied to two observed samples of cluster peculiar velocities: the SCI sample (Giovanelli et al. 1997) and a subsample of the Mark III catalogue (Willick et al. 1997). Watkins (1997) found that the rms one-dimensional cluster peculiar velocity is 256^{+106}_{-75} km s^{-1}, which corresponds to the three-dimensional rms velocity 459^{+184}_{-130} km s^{-1} . Dale et al. (1999) obtained Tully-Fisher peculiar velocities for 52 Abell clusters distributed over the whole the sky between ~ 50 and $\sim 200h^{-1}$ Mpc. They found that the rms one-dimensional cluster peculiar velocity is 341 ± 93 km s^{-1}, which corresponds to the three-dimensional rms velocity 591 ± 161 km s^{-1}.

Radial peculiar velocities of clusters can be determined to large distances measuring the Sunyaev-Zeldovich (1980) (SZ) effect. Rephaeli & Lahav (1991) made one of the first estimates of the possibility of measuring the peculiar velocities by using the SZ effect for a selected sample of galaxy clusters. However, most convincing measurements for individual clusters have been done only recently, using the new generation of sensitive bolometers (Holzapfel et al. 1997; Lamarre et al. 1998). The accuracy of SZ measurements for determining the peculiar velocities of clusters by the Planck satellite was studied by Aghanim, Gorski, Puget (2000).

In this paper we study the rms peculiar velocity of clusters, v_{rms}, in different cosmological models assuming that the initial density fluctuation field is a Gaussian field. To in-

vestigate the nonlinear regime, we use N-body simulations. We examine cluster peculiar velocities for different cluster masses. Do cluster velocities depend on their masses? The rms peculiar velocity of peaks in the initial Gaussian field does not depend on the height of peaks (Bardeen et al. 1986). However, as an initially Gaussian density field evolves gravitationally in the nonlinear regime, it becomes non-Gaussian.

The evolution of peculiar velocities of galaxy clusters in different N-body models with an initially Gaussian density field has been examined in several papers (e.g. Bahcall, Gramann, Cen 1994; Croft & Efstathiou 1994; Suhhonenko & Gramann 1999, Colberg et al 2000; Sheth & Diaferio 2001). Groth & Efstathiou (1994) studied the cluster peculiar velocities for two different cluster richnesses,described by the mean intercluster separations $d_{cl} = 30h^{-1}$ Mpc and $d_{cl} = 55h^{-1}$ Mpc. They found that the peculiar velocity distributions are almost independent of cluster richness. Sheth & Diaferio (2001) studied rms peculiar velocity of clusters for different masses and found that in N-body simulations the rms velocity of clusters depends only weakly on cluster mass, with a small trend that for more massive clusters the rms peculiar velocity decreases. On the other hand, Suhhonenko & Gramann (1999) investigated the properties of clusters using N-body simulations and found that the rms peculiar velocities of clusters increase with cluster richness. The rms peculiar velocity of small clusters was similar to the linear theory expectations, while the rms peculiar velocity of rich clusters was higher than that predicted in the linear theory (≈ 18 per cent for clusters with the mean intercluster separation $d_{cl} = 30h^{-1}$ Mpc).

In this paper we study the dependence of v_{rms} on cluster masses in more detail. We also examine the rms peculiar velocities of clusters for different cluster radii. We use the N-body simulations published by the Virgo Consortium and described in detail by Jenkins et al. (1998). These simulations were carried out using a parallel, adaptive particle-particle/particle-mesh ($\mathrm{AP^3M}$) code (Couchman, Thomas & Pearce 1995; Pearce & Couchman 1997). In this paper we analyze the velocities in the ΛCDM and τCDM model (see Jenkins et al. (1998) and Section 2 for the description of the cosmological parameters in these models). We also follow the evolution of particles in the similar ΛCDM model with the same cosmological parameters but using a particle-mesh (PM) code (with the same mass resolution adopted in the Virgo simulations used in this paper).

This paper is organized as follows. In Section 2 we describe the cosmological models, N-body simulations and cluster selection algorithms used. We also examine the linear theory predictions for the peculiar velocities of peaks in the Gaussian field. In Section 3 we examine the rms peculiar velocity of clusters for different cluster masses and radii, and compare the cluster velocities with the linear theory predictions. A summary and discussion are presented in Section 4.

2 MODELS

2.1 Simulations

We analyze peculiar velocities in N-body simulations carried out by the Virgo consortium for two cosmological models, ΛCDM ($\Omega_0 = 0.3$, $\Lambda = 0.7$) and τCDM ($\Omega_0 = 1$) as described by Jenkins et al. (1998). In these cold dark matter (CDM) models the power spectrum of the initial conditions was chosen to be in the form given by Bond & Efstathiou (1984),

$$P(k) = \frac{Ak}{[1 + (aq + (bq)^{3/2} + (cq)^2)^\nu]^{2/\nu}}, \qquad (1)$$

where $q = k/\Gamma$, $a = 6.4h^{-1}$ Mpc, $b = 3h^{-1}$ Mpc, $c = 1.7h^{-1}$ Mpc, $\nu = 1.13$ and $\Gamma = 0.21$. The normalization constant, A, was chosen by fixing the value of σ_8 (the linearly extrapolated mass fluctuation in spheres of radius $8h^{-1}$ Mpc); $\sigma_8 = 0.9$ and $\sigma_8 = 0.51$ for the ΛCDM and τCDM model, respectively.

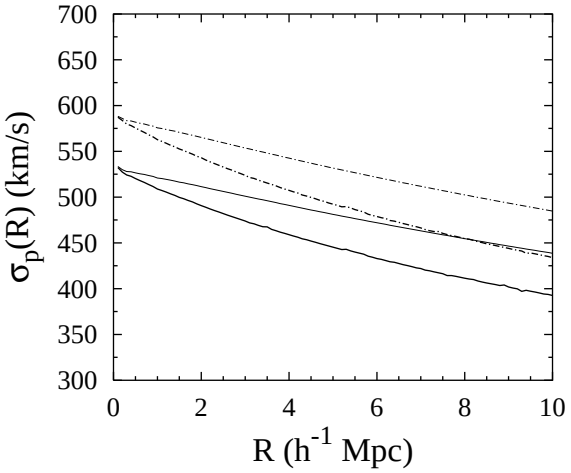

Figure 1. The rms peculiar velocity of peaks, $\sigma_p(R)$, in the ΛCDM model with $\Omega_0 = 0.3$ and $\sigma_8 = 0.9$ (heavy solid line) and in the τCDM model with $\Omega_0 = 1.0$ and $\sigma_8 = 0.51$ (heavy dot-dashed line). The light curves show the corresponding rms peculiar velocity $\sigma_v(R)$ for the same models.

We investigated the linear theory predictions for peculiar velocities of peaks in the ΛCDM and τCDM model. The linear rms velocity fluctuation on a given scale R can be expressed as

$$\sigma_v(R) = H_0 f(\Omega_0)\sigma_{-1}(R), \qquad (2)$$

where spectral moments σ_j are defined for any integer j by

$$\sigma_j^2 = \frac{1}{2\pi^2}\int P(k)W^2(kR)k^{2j+2}dk, \qquad (3)$$

$W^2(kR)$ is a window function and $f(\Omega_0)$ is the dimensionless growth rate. The function $f(\Omega_0) = 0.51$ and $f(\Omega_0) = 1.0$ in the ΛCDM and τCDM model, respectively. (We note that the approximation $f(\Omega_0) = \Omega_0^{0.6}$ underestimates the dimensionless growth rate by $\sim 5\%$ in the flat $\Omega_0 = 0.3$ model).

Bardeen et al. (1986) showed that in the linear approximation the rms peculiar velocity at peaks of the smoothed density field differs systematically from $\sigma_v(R)$, and can be expressed as

$$\sigma_p(R) = \sigma_v(R)\sqrt{1 - \sigma_0^4/\sigma_1^2\sigma_{-1}^2}. \qquad (4)$$

In this approximation, the rms velocities of peaks do not depend on the height of the peaks.

Fig. 1 shows the rms peculiar velocity of peaks, $\sigma_p(R)$,

for the ΛCDM and τCDM model. We have used the top-hat window function. For comparison, we show also the rms peculiar velocity $\sigma_v(R)$ for the same models. For the radius $R = 1h^{-1}$ Mpc, σ_p is lower than σ_v about ~ 2.3 and ~ 2.2 per cent for the ΛCDM and τCDM model, respectively. On larger scales, the difference between σ_p and σ_v increases.

Next we study peculiar velocities in N-body simulations. The Virgo simulations were created using a parallel adaptive particle-particle/particle-mesh (AP^3M) code as described by Couchman, Thomas & Pearce (1995) and Pearce & Couchman (1997). It supplements the standard P^3M algorithm (Efstathiou et al. 1985) by recursively placing higher resolution meshes, 'refinements', in heavily clustered regions. The Virgo simulations were done on two large Cray T3D parallel supercomputers at Edinburgh Parallel Computing Center and at the Computing Center of the Max Plank Society in Garching. These simulations are publicly available at *http://www.mpa-garching.mpg.de/Virgo/virgoproject.html.*

In the simulations used here, the evolution of particles was followed in the comoving box of size $L = 239.5h^{-1}$ Mpc. The number of particles was $N_p = 256^3$. Therefore, the mean particle separation $\lambda_p = L/N_p^{1/3} = 0.9355h^{-1}$ Mpc. The mean separation λ_p determines the mass resolution scale in the simulations. The mass of the particle $m_p = \rho_b\lambda_p^3 = 6.82 \times 10^{10}h^{-1}M_\odot$ and $m_p = 2.27 \times 10^{11}h^{-1}M_\odot$ in the ΛCDM and τCDM models, respectively (here ρ_b is the mean background density). The gravitational softening length is $r_{soft} = 25h^{-1}$ kpc and $r_{soft} = 36h^{-1}$ kpc , respectively (see Jenkins et al. (1998) for a detailed description of the force calculation scheme used in the Virgo simulations).

We also investigated the evolution of 256^3 particles on a 256^3 grid using a particle-mesh (PM) code described by Gramann (1988) and Suhhonenko & Gramann (1999). The PM method is discussed in detail by Hockney & Eastwood (1981) and Efstathiou et al.(1985). The cosmological parameters for this simulation were chosen similar to the ΛCDM model. We chose the flat $\Omega_0 = 0.3$ model and used the initial power spectrum $P(k)$ given in eq. (1) (with $\sigma_8 = 0.9$). The comoving box size was $L = 239.5h^{-1}$ Mpc. Therefore, the mean particle separation, λ_p, and the mass of the particle, m_p, in this model are the same as used in the Virgo ΛCDM model. We denote this model as the PM model.

We examined the rms velocity of particles in the simulations studied. In the ΛCDM and τCDM models, the rms velocity of particles was 648 km s^{-1} and 636 km s^{-1}, respectively. In the PM model, the rms velocity was 585 km s^{-1}. Due to the small-scale smoothing inherent to the PM method, the intrinsic velocity dispersions of clusters in the PM model are smaller than in the ΛCDM model. The velocity field of clusters in these models is expected to be similar.

2.2 Selection of clusters

We used two different algorithms to identify clusters in simulations: the standard friends-of-friends (FOF) algorithm, and the algorithm, where clusters are defined as maxima of the density field smoothed on the scale $R \sim 1h^{-1}$ Mpc (DENSMAX).

The friends-of-friends group finder algorithm was applied using the suit of program developed by the cosmology group in the University of Washington. These programs are available at *http://www-hpcc.astro.washington.edu.*

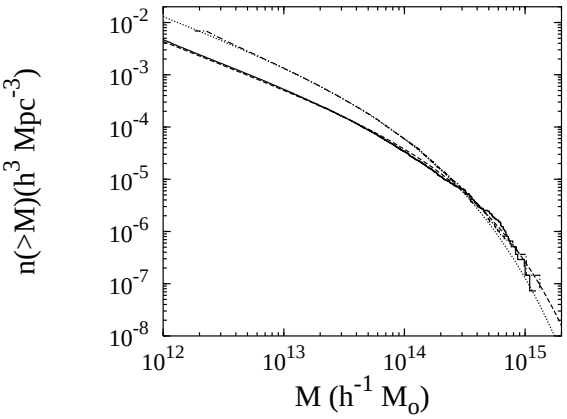

Figure 2. The cluster mass function in the Virgo ΛCDM model for the parameter $b = 0.164$ (solid line) and in the τCDM model for $b = 0.2$ (dot-dashed line). For comparison we show the fitting formulae given by Jenkins et al. (2001) for the mass function in the ΛCDM (dashed line) and in the τCDM model (dotted line).

The FOF cluster finder depends on one parameter b, which defines the linking length as $b\lambda_p$. The conventional choice for this parameter is $b = 0.2$ (see e.g. Götz, Huchra & Brandenberger 1998; Jenkins et al. 2001). In this paper we also define clusters by using the value $b = 0.2$. We also study velocities of the clusters defined by the parameter $b = 0.15$ and $b = 0.3$.

To test our FOF output data, we found the mass function of clusters in the Virgo simulations. The cluster mass function in these simulations has been studied in detail by Jenkins et al. (2001). Fig. 2 shows the mass function of clusters determined for $b = 0.164$ in the ΛCDM model and for $b = 0.2$ in the τCDM model. For comparison we show the mass functions given by the approximations obtained by Jenkins et al. (2001) (eq. (B2) and (B1) for the ΛCDM and τCDM model, respectively). Jenkins et al. (2001) studied the mass function at the high mass end up to the point where the predicted Poisson abundance errors reach 10%. In the simulations studied here, this limit is reached when $n = 7.3\times10^{-6}\,h^3\,\mathrm{Mpc}^{-3}$. Fig. 2 shows that if n is larger than this value, the agreement between our results and these obtained by Jenkins et al. (2001) is very good.

We studied clusters that contained at least ten particles. The three-dimensional velocity of each cluster was defined as

$$\vec{v}_{cl} = \frac{1}{N_p}\sum_{i=1}^{N_p}\vec{v}_i, \qquad (5)$$

where N_p is the number of particles in the cluster and $\vec{v}_i$ is the velocity of the particle i in the cluster. To characterize the size of the cluster, we use the effective radius defined as

$$R_{eff}^2 = \frac{1}{N_p}\sum_{i=1}^{N_p}\left[(x_i-\bar{x})^2 + (y_i-\bar{y})^2 + (z_i-\bar{z})^2\right], \qquad (6)$$

where x_i, y_i, z_i are the particle coordinates in the cluster and $(\bar{x}, \bar{y}, \bar{z})$ are the coordinates of the cluster centre.

We also selected clusters by using the DENSMAX method. In this case clusters were identified in the simulations as maxima of the density field that was determined on a 256^3 grid using the cloud-in-cell (CIC) scheme. To determine peculiar velocities of clusters, v_{cl}, we calculated the peculiar velocity field on a 256^3 grid using the CIC-scheme, and found peculiar velocities at the grid points where the clusters had been identified. If we use the DENSMAX method, the size of the selected clusters is similar for all clusters, and given by the cell grid size, λ_g. In our case, the cell size $\lambda_g = 0.9355h^{-1}$ Mpc.

To determine the rms peculiar velocities of clusters, we used the equation

$$v_{rms}^2 = v_s^2 + v_L^2 = \frac{1}{N_{cl}} \sum_{i=1}^{N_{cl}} v_{cli}^2 + v_L^2, \qquad (7)$$

where the parameter v_s describes the dispersion of cluster velocities, v_{cli}, derived from simulation and the parameter v_L is given by

$$v_L^2 = \frac{f^2(\Omega_0) H_0^2}{2\pi^2} \int_0^{\frac{2\pi}{L}} P(k) dk. \qquad (8)$$

N_{cl} is the number of clusters studied. For ΛCDM and τCDM models, we found that $v_L = 220$ km s^{-1} and $v_L = 245$ km s^{-1}, respectively.

Table 1. The number of clusters, N_{cl}, in the different density and mass intervals. N_{cl} in the different density intervals is given for the clusters selected with the DENSMAX method. N_{cl} in the different mass intervals is given for the clusters determined with the FOF method with $b = 0.2$.

ρ/ρ_b	N_{cl} ΛCDM	N_{cl} τCDM	N_{cl} PM
1 – 5	148496	169774	112674
5 – 10	29265	35753	20842
10 – 50	31294	34705	22171
50 – 100	5246	4015	3496
100 – 500	4253	1762	1980
500 – 1000	298	22	48
1000 – 5000	78	0	3
M ($h^{-1}M_\odot$)	N_{cl} ΛCDM	N_{cl} τCDM	N_{cl} PM
5×10^{11} – 10^{12}	36227	0	19213
10^{12} – 5×10^{12}	51841	57460	25000
5×10^{12} – 10^{13}	7326	19298	3755
10^{13} – 5×10^{13}	6542	15489	3804
5×10^{13} – 10^{14}	856	1644	573
10^{14} – 5×10^{14}	511	789	358
5×10^{14} – 10^{15}	38	18	25
10^{15} – 5×10^{15}	4	5	4

3 RESULTS

We investigated the rms velocity of clusters in different density and mass intervals. The results are presented in Fig. 3. The clusters defined with the DENSMAX method were divided into subgroups according to their density. We studied the rms velocity of clusters in seven subgroups, where the density ρ/ρ_b was in the range $1-5$, $5-10$, $10-50$,...,$1000-5000$. Table 1 shows the number of clusters and the upper right panel in Fig. 3 shows the rms velocity of clusters in the different density intervals. We see that in the AP^3M ΛCDM and τCDM models, the rms velocity of clusters is almost independent of the density. The rms velocity somewhat increases at smaller densities. However, this increase is small (≈ 10 per cent). On the other hand, in the PM model the rms velocity increases significantly with density. The rms velocity is 450 km s^{-1} for the low-density clusters in the range $\rho/\rho_b = 1-5$ and 800 km s^{-1} for the high-density clusters in the range $\rho/\rho_b = 500-1000$.

The clusters determined with the FOF method were divided into subgroups according to their mass. We studied the rms velocity of clusters in eight subgroups, where the mass was in the range $(5\times10^{11}-10^{12})h^{-1}M_\odot$, ..., $(10^{15}-5\times10^{15})h^{-1}M_\odot$. Table 3 shows the number of clusters and Fig. 3 demonstrates the rms peculiar velocity of clusters in the different mass intervals. The lower right panel in Fig. 3 shows the results for the clusters determined by $b = 0.2$. The left panels show the rms velocities of clusters defined by $b = 0.15$ and $b = 0.3$.

We see that in the AP^3M ΛCDM and τCDM models, the rms velocity somewhat decreases with cluster mass. In the ΛCDM model for $b = 0.2$, the rms velocity of clusters is 525 km s^{-1} in the mass interval $(5\times10^{11}-10^{12})h^{-1}M_\odot$ and 430 km s^{-1} in the mass interval $(10^{15}-5\times10^{15})h^{-1}M_\odot$. For $b = 0.15$ and $b = 0.3$, this effect is similar. These results are in good agreement with the results obtained by Sheth & Diaferio (2001). They studied the rms velocities of clusters in different mass intervals and found that the rms cluster velocity decreases with mass. Sheth & Diaferio (2001) also used Virgo simulations in their study.

If we consider the rms velocity of clusters in the PM model, we see that the rms velocity for massive clusters increases. For $b = 0.2$, the rms velocity of clusters is 585 km s^{-1} in the range $(5\times10^{11}-10^{12})h^{-1}M_\odot$ and it increases to 835 km s^{-1} in the range $(5\times10^{14}-10^{15})h^{-1}M_\odot$. For the parameter $b = 0.15$, this effect is somewhat larger, and for $b = 0.3$ smaller (see Fig. 3 for details).

We also studied the rms velocity of clusters with density (or mass) higher than a given threshold density (or mass). The results are presented in Fig. 4. The DENSMAX clusters were ranked according to their density, and we selected $N_{cl} = (L/d_{cl})^3$ highest ranked clusters to produce cluster catalogues with a mean intercluster separation $10-50h^{-1}$ Mpc. Similarly, the FOF clusters were ranked according to their mass. Table 2 shows the density and mass thresholds used to produce the cluster catalogues for different values of the mean cluster separation. For comparison, the number density of observed APM clusters and Abell clusters is $n_{cl} \sim 3.4\times10^{-5}h^3$ Mpc^{-3} ($d_{cl} \sim 31h^{-1}$Mpc) and $n_{cl} \sim 2.5\times10^{-5}h^3$ Mpc^{-3} ($d_{cl} \sim 34h^{-1}$ Mpc), respectively (Dalton et al. 1994, Einasto et al. 1997).

Fig. 4 demonstrates the rms peculiar velocity of clusters with a mean separation $d_{cl} = 10-50h^{-1}$ Mpc. In this range, the rms velocity of DENSMAX clusters in the AP^3M ΛCDM and τCDM models is almost independent of the density of clusters. For the clusters with a mean

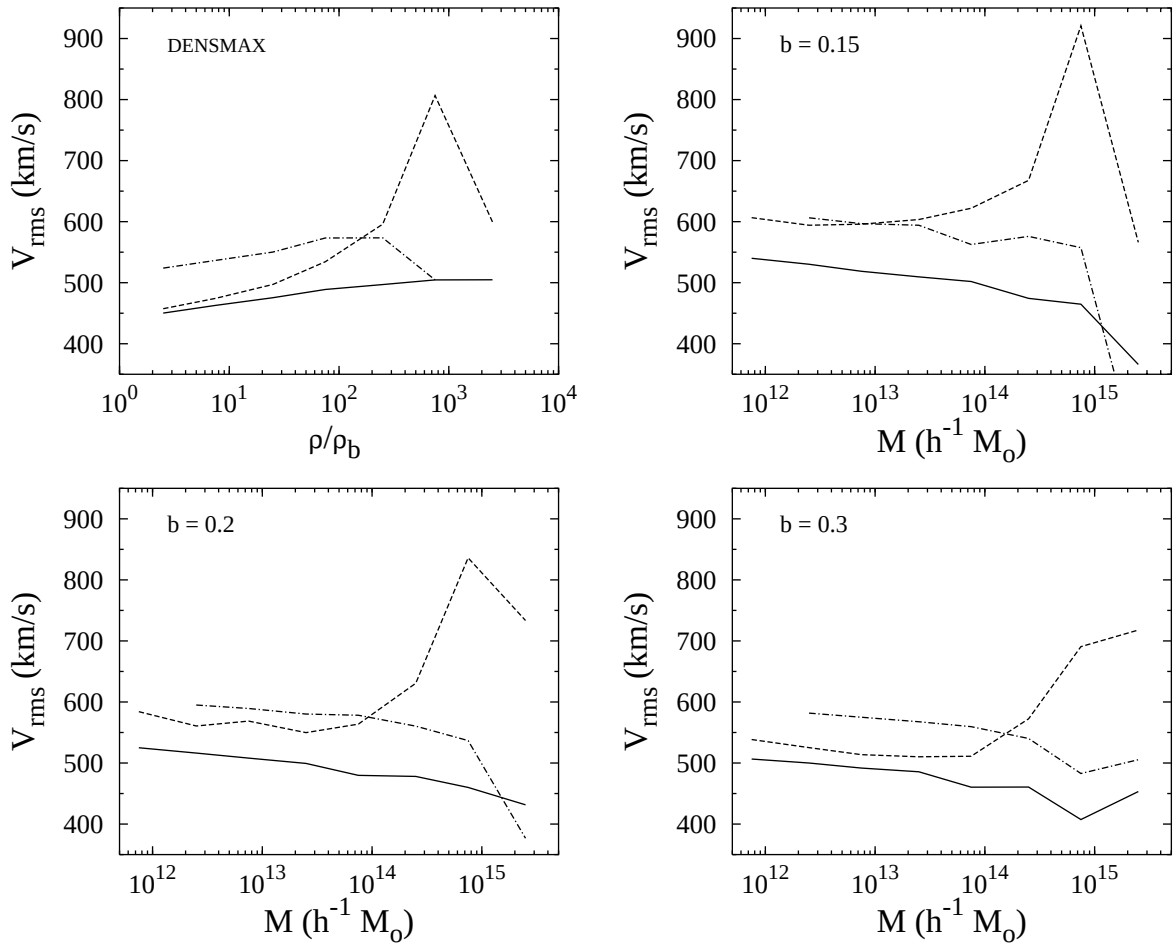

Figure 3. The rms peculiar velocities of clusters for different densities and masses in the AP^3M ΛCDM model (solid lines), τCDM model (dot-dashed lines) and in the PM model (dashed lines). The upper right panel shows the results for the clusters defined by the DENSMAX method and the lower right panel shows the results for the clusters selected by the FOF method with $b = 0.2$. The left panels show the rms velocities of clusters defined by the FOF method with $b = 0.15$ and $b = 0.3$, respectively.

Table 2. The Density and mass thresholds used to produce the cluster catalogues with a mean separation $d_{cl} = 10 - 50h^{-1}$ Mpc. The mass thresholds are given for the FOF clusters determined by $b = 0.2$.

d_{cl} (h^{-1} Mpc)	ρ_t/ρ_b ΛCDM	ρ_t/ρ_b τCDM	ρ_t/ρ_b PM
10	35	27	22
20	213	102	110
30	435	178	199
40	652	254	297
50	850	315	381

d_{cl} (h^{-1} Mpc)	M_t (ΛCDM) ($h^{-1}M_\odot$)	M_t (τCDM) ($h^{-1}M_\odot$)	M_t (PM) ($h^{-1}M_\odot$)
10	5.6×10^{12}	1.3×10^{13}	2.8×10^{12}
20	4.3×10^{13}	6.4×10^{13}	3.0×10^{13}
30	1.1×10^{14}	1.3×10^{14}	8.2×10^{13}
40	2.0×10^{14}	2.0×10^{14}	1.6×10^{14}
50	3.0×10^{14}	2.8×10^{14}	2.3×10^{14}

separation $d_{cl} = 30h^{-1}$ Mpc, $v_{rms} = 510$ km s^{-1} and $v_{rms} = 580$ km s^{-1} in the ΛCDM and τCDM models, respectively. The rms velocity of FOF clusters in these models decreases with cluster richness. In the ΛCDM model for $b = 0.2$, the rms velocities are 500 km s^{-1} and 430 km s^{-1}, if $d_{cl} = 10h^{-1}$ Mpc and $d_{cl} = 50h^{-1}$ Mpc, respectively. For $b = 0.15$ and $b = 0.3$, this effect is similar. For the clusters with $d_{cl} = 30h^{-1}$ and $b = 0.2$, $v_{rms} = 475$ km s^{-1} and $v_{rms} = 565$ km s^{-1} in the ΛCDM and τCDM models, respectively.

Contrary, in the PM model, the rms peculiar velocities increase with the number density density of clusters and their mass. In this model for the parameter $b = 0.2$, the rms velocities are 560 km s^{-1} and 735 km s^{-1}, if $d_{cl} = 10h^{-1}$ Mpc and $50h^{-1}$ Mpc, respectively. For the mean separation $d_{cl} = 30h^{-1}$ Mpc, $v_{rms} = 685$ km s^{-1} for the DENSMAX clusters and $v_{rms} = 630$ km s^{-1} for the FOF clusters with $b = 0.2$.

Our results are in good agreement with the results obtained by Colberg et al. (2000). They also studied the rms velocity of clusters in the AP^3M ΛCDM and τCDM models, but used a slightly different method to select clusters.

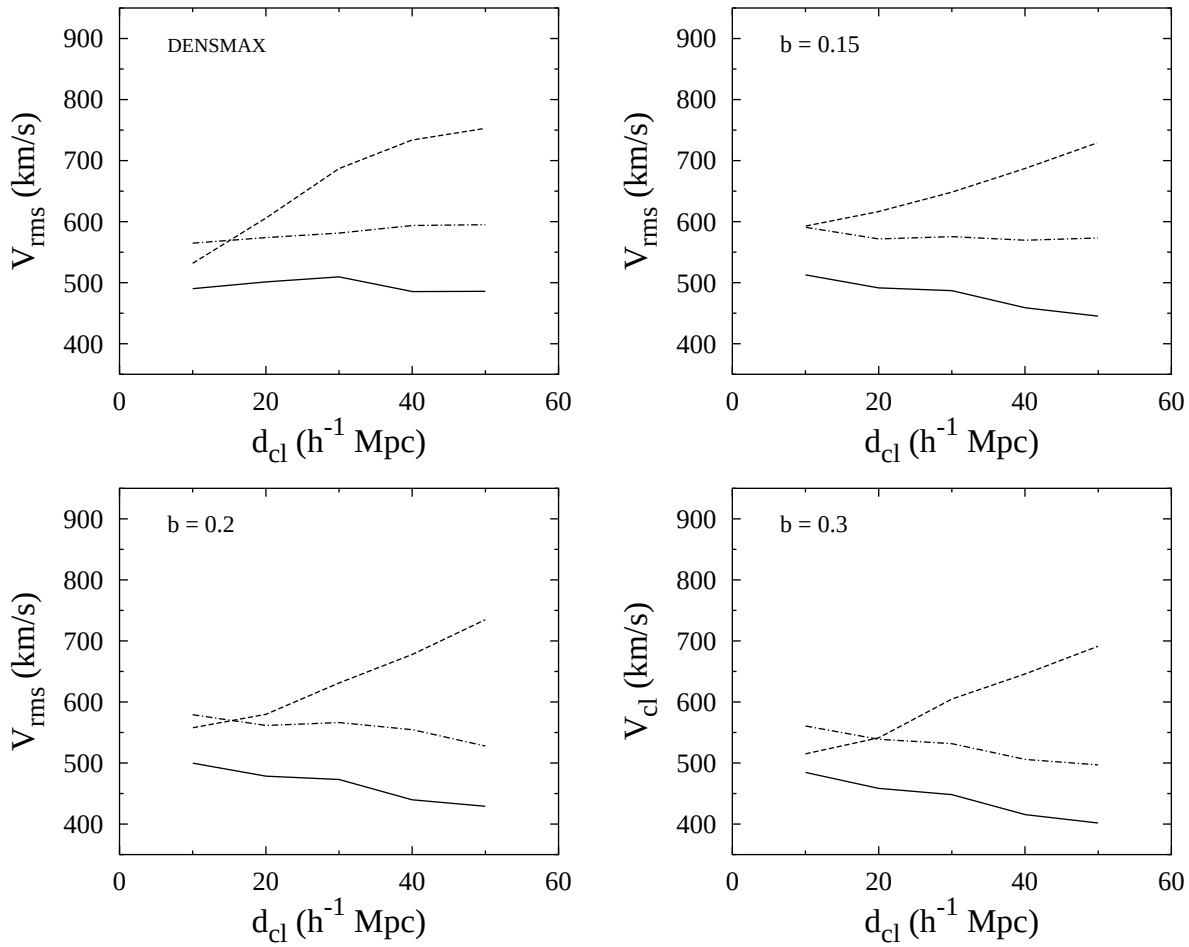

Figure 4. The rms peculiar velocities of clusters for different values of the mean cluster separation, d_{cl}. The clusters are ranked according to their density (DENSMAX clusters) or mass (FOF clusters). The lines are coded as in Fig. 3.

High-density regions were located using a FOF method with $b = 0.05$ and their barycentres were considered as candidate cluster centers. Any candidate centre for which mass within $1.5h^{-1}$ Mpc exceeded threshold mass M_t was identified as a candidate cluster. The final cluster list was obtained by deleting the lower mass candidate in all pairs separated by less than $1.5h^{-1}$ Mpc. The peculiar velocity of each cluster was defined to be the mean peculiar velocity of all the particles within the $1.5h^{-1}$ Mpc sphere. In this method, the size of the selected clusters is same for all clusters and in this sense, this method is similar to the DENSMAX method.

Colberg et al. (2000) used the value $M_t = 3.5 \times 10^{14}h^{-1}M_\odot$. For this value, the number of clusters was ≈ 70 in the ΛCDM and τCDM model ($d_{cl} \approx 58h^{-1}$Mpc). They found that the rms velocity of these clusters, v_s are 439 km s^{-1} and 535 km s^{-1} in the AP^3M λCDM and τCDM models, respectively (they did not include the dispersion v_L^2). If we use the DENSMAX method, we find that in the Virgo simulations the rms velocity of clusters is almost independent of the number density of clusters and for $d_{cl} = 50h^{-1}$ Mpc, the velocities are $v_s = 450$ km s^{-1} and 549 km s^{-1} in the ΛCDM and τCDM models, respectively. These values are very close to the values found by Colberg et al. (2000), [hit slightly larger (≈ 2 per cent). This small difference is probably caused by the fact that in the DENSMAX method we use the smoothing length $1h^{-1}$ Mpc, which is smaller than $1.5h^{-1}$Mpc]. For comparison, the velocity v_s, for the FOF clusters with $b = 0.2$ and $d_{cl} = 50h^{-1}$ Mpc, is 368 km s^{-1} and 468 km s^{-1} in the ΛCDM and τCDM modelS, respectively.

Let us now consider the rms velocities of clusters for different cluster radii. We studied the rms velocity of clusters with effective radius R_{eff} larger than a given threshold radius. The clusters were ranked according to their effective radius and we selected $N_{cl} = (L/d_{cl})^3$ highest ranked clusters to produce cluster catalogues with mean separations $10 - 50h^{-1}$ Mpc. Table 3 shows the threshold radii used for different values of the mean cluster separation.

Fig. 5 ilustrates the dependence of v_{rms} on cluster radii. We see that the effect of cluster radius on v_{rms} is similar to the effect of cluster mass on v_{rms} (compare Fig. 4 and Fig. 5). In the AP^3M ΛCDM and τCDM models, the rms velocity of small clusters is somewhat higher than the rms velocity of large clusters. For example, in the ΛCDM model for $b = 0.2$, the rms velocities are 520 km s^{-1} and 450 km s^{-1} for the clusters with $d_{cl} = 10h^{-1}$ Mpc and $d_{cl} = 50h^{-1}$ Mpc, respectively. In the PM model, the rms velocities of clusters increase with the cluster effective radius. For the clusters

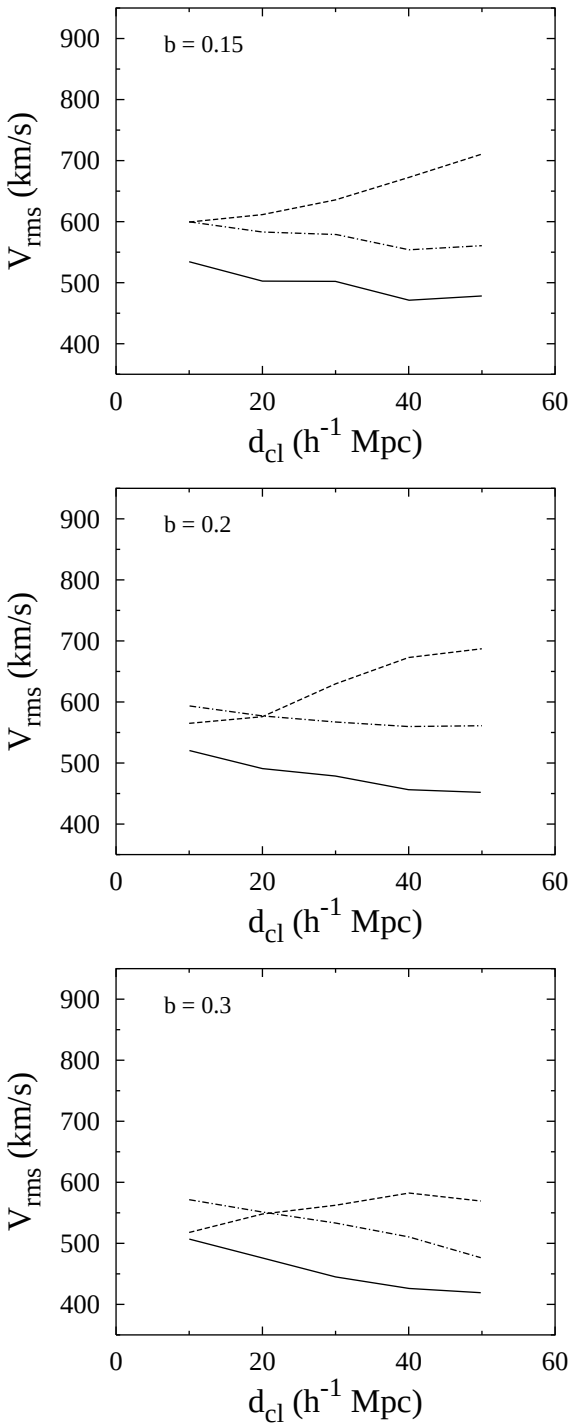

Figure 5. The rms peculiar velocities of clusters for different values of the mean cluster separation, d_{cl}. The clusters are ranked according to their effective radius, R_{eff}. The lines are specified similarly to the Fig.3. The upper panel shows the velocities for the clusters defined with $b = 0.15$, the middle panel for the clusters defined with $b = 0.2$ and lower panel for the clusters defined with $b = 0.3$.

Table 3. The threshold radii R_t used to produce the cluster catalogues with a mean separation $d_{cl} = 10 - 50h^{-1}$ Mpc. The radii are given for the FOF clusters defined by $b = 0.2$.

d_{cl} (h^{-1} Mpc)	R_t (ΛCDM) (h^{-1} Mpc)	R_t (τCDM) (h^{-1} Mpc)	R_t (PM) (h^{-1} Mpc)
10	0.22	0.24	0.29
20	0.40	0.40	0.67
30	0.58	0.53	0.99
40	0.74	0.64	1.23
50	0.88	0.72	1.40

Table 4. Comparison of the rms velocity of clusters, v_{rms}, with the linear theory predictions for peculiar velocities of peaks, σ_p, for the radius $R = 1h^{-1}$ Mpc. The results are given for the FOF clusters determined by $b = 0.2$.The clusters are ranked according to their mass.

d_{cl} (h^{-1} Mpc)	v_{rms}/σ_p ΛCDM	v_{rms}/σ_p τCDM	v_{rms}/σ_p PM
10	0.98	1.03	1.10
30	0.93	1.01	1.24
50	0.84	0.94	1.44

defined by the parameter $b = 0.3$, this effect is smaller than for the clusters defined by $b = 0.15$ and $b = 0.2$ (see Fig. 5).

We can compare cluster velocities in N-body simulations with the linear theory predictions for peculiar velocities of peaks, $\sigma_p(R)$. In Table 4 we compare the rms velocity of clusters, v_{rms}, with $\sigma_p(R)$ for the radius $R = 1h^{-1}$ Mpc. At this radius, $\sigma_p = 509$ km/s and $\sigma_p = 562$ km/s in the ΛCDM and τCDM models, respectively. We analyzed the rms velocity of FOF clusters for different values of the cluster separation. The clusters were ranked according to their mass. The results are given for the clusters determined with $b = 0.2$. The rms peculiar velocities v_{rms} for the clusters determined by $b = 0.15$ and $b = 0.3$ are similar (Fig. 4). In the AP^3M ΛCDM model, the rms peculiar velocity of small clusters is close to the linear theory expectations, while the rms peculiar velocity of rich clusters is smaller ($\approx 16\%$ per cent for clusters with a mean intercluster separation $d_{cl} = 50h^{-1}$ Mpc). In the PM model, the rms velocity of rich clusters is substantially higher than predicted ($\approx 44\%$ for the clusters with $d_{cl} = 50h^{-1}$ Mpc).

4 SUMMARY AND DISCUSSION

In this paper we have examined the rms peculiar velocities of galaxy clusters for different cluster masses and radii. We analyzed clusters in the Virgo simulations for two cosmological models, ΛCDM and τCDM (Jenkins et al. 1998). These simulations were carried out using the AP^3M code. We used the simulations where the mean particle separation $\lambda_p \sim 1h^{-1}$ Mpc. We also analyzed clusters in an N-body simulation where the evolution was followed using a PM code with the same mass resolution that was used in the Virgo simulations. The cosmological parameters for this simulation were chosen similar to the Virgo ΛCDM model.

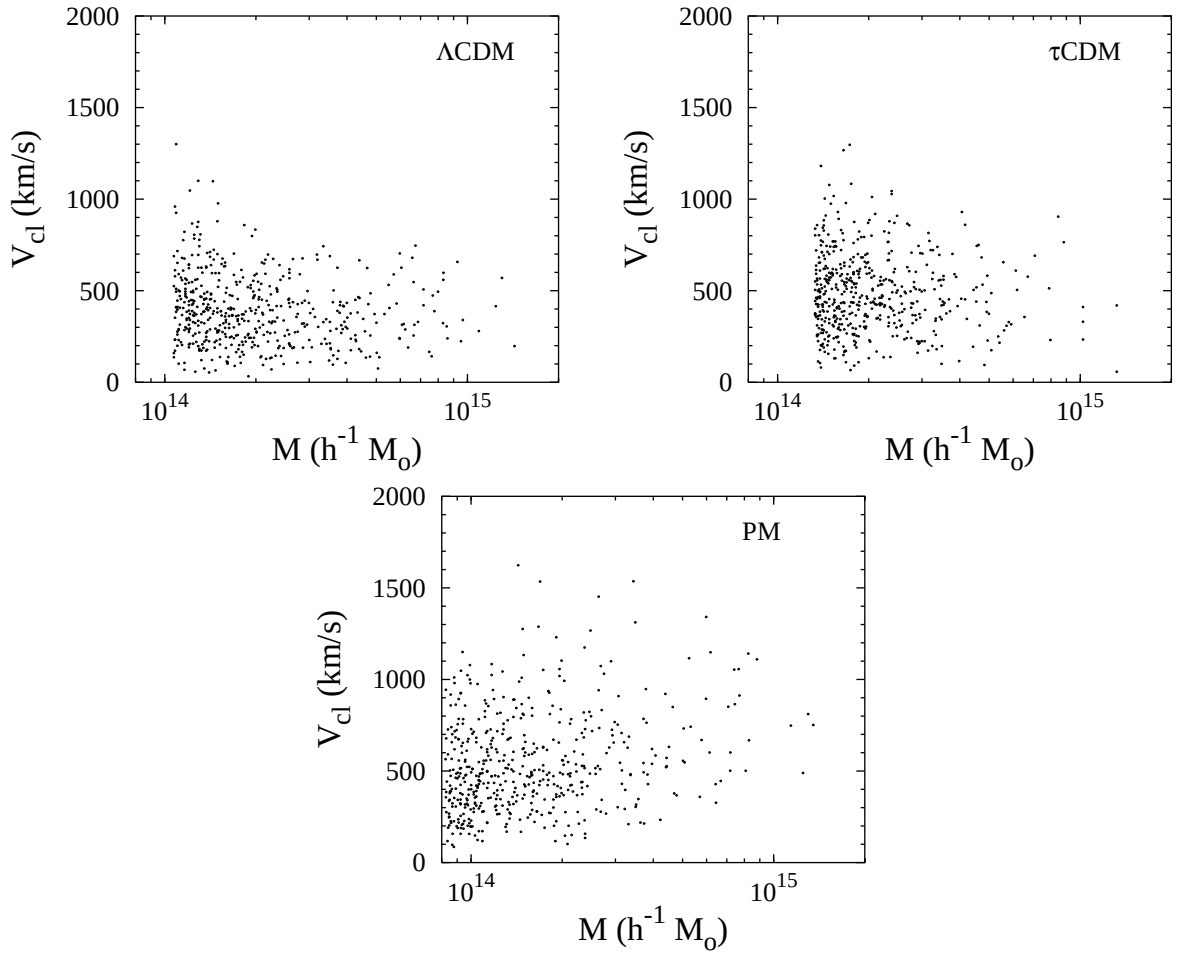

Figure 6. The peculiar velocity of a cluster, v_{cl}, vs. the mass of the cluster, M, for the 509 most massive clusters ($d_{cl} = 30\,h^{-1}\,\mathrm{Mpc}$). The clusters are defined using the FOF method with $b = 0.2$. The upper panel shows the velocities in the AP^3M ΛCDM model, the middle panel in the τCDM model, and the lower panel in the PM model.

To identify clusters in the simulations we used two methods: the standard friends-of-friends (FOF) method and the method where the clusters are defined as maxima of the density field smoothed on the scale $R \sim 1h^{-1}$ Mpc. The rms velocities of the selected clusters were compared with the linear theory predictions for the rms peculiar velocities of peaks for the smoothing radius $R = 1h^{-1}$ Mpc.

We found that in the AP^{3}M simulations the rms velocity of clusters defined with the DENSMAX method is almost independent of the number density of cluster. For the clusters with a mean separation $d_{cl} = 30h^{-1}$ Mpc, $v_{rms} = 510\ \mathrm{km\,s^{-1}}$ and $v_{rms} = 580\ \mathrm{km\,s^{-1}}$ in the ΛCDM and τCDM models, respectively. The rms velocity of FOF clusters decreases with cluster mass and radius. In the ΛCDM model, the rms peculiar velocity of massive clusters with an intercluster separation $d_{cl} = 50h^{-1}$ Mpc is $\approx 15\%$ smaller than the rms velocity of clusters with a separation $d_{cl} = 10h^{-1}$ Mpc. For the clusters defined by $b = 0.2$ and $d_{cl} = 30h^{-1}$, the $v_{rms} = 475\ \mathrm{km\,s^{-1}}$ and $v_{rms} = 565\ \mathrm{km\,s^{-1}}$ in the ΛCDM and τCDM model, respectively.

Contrary, in the PM simulation, the peculiar velocities of massive clusters are higher than the peculiar velocities of low-mass clusters. In this simulation, the rms velocity of massive clusters is $\sim 30\%$ higher than the rms velocity of clusters with a separation $d_{cl} = 10h^{-1}$ Mpc. For $d_{cl} = 30h^{-1}$ Mpc, the rms peculiar velocity is $685\ \mathrm{km\,s^{-1}}$ for the DENSMAX clusters and $630\ \mathrm{km\,s^{-1}}$ for the FOF clusters with $b = 0.2$.

In Fig. 6 we plot the peculiar velocities of clusters, v_{cl}, versus the mass of the cluster, M. The velocities are shown for the 509 most massive clusters with a mean separation $d_{cl} = 30h^{-1}$ Mpc ($M_t = 1.1 \times 10^{14}$, 1.3×10^{14}, and $8.2 \times 10^{13} h^{-1} M_\odot$ in the ΛCDM, τCDM model and PM model, respectively.) The clusters are determined using the FOF method with the parameter $b = 0.2$. We see that the distribution of cluster velocities in the AP^3M ΛCDM and PM models is different. In the AP^3M ΛCDM model, all the clusters with masses $M > 2 \times 10^{14} h^{-1} M_\odot$ have velocities $v_{cl} < 800\ \mathrm{km\,s^{-1}}$. In the PM model, there are many massive clusters which move with speeds $v_{cl} > 800\ \mathrm{km\,s^{-1}}$. In this model, there are only few clusters with masses $M > 4 \times 10^{14} h^{-1} M_\odot$ and with velocities $v_{cl} < 400\ \mathrm{km\,s^{-1}}$.

We studied also the intrinsic velocity dispersion, σ^2_{cl}, in the massive clusters. The intrinsic velocity dispersion of the

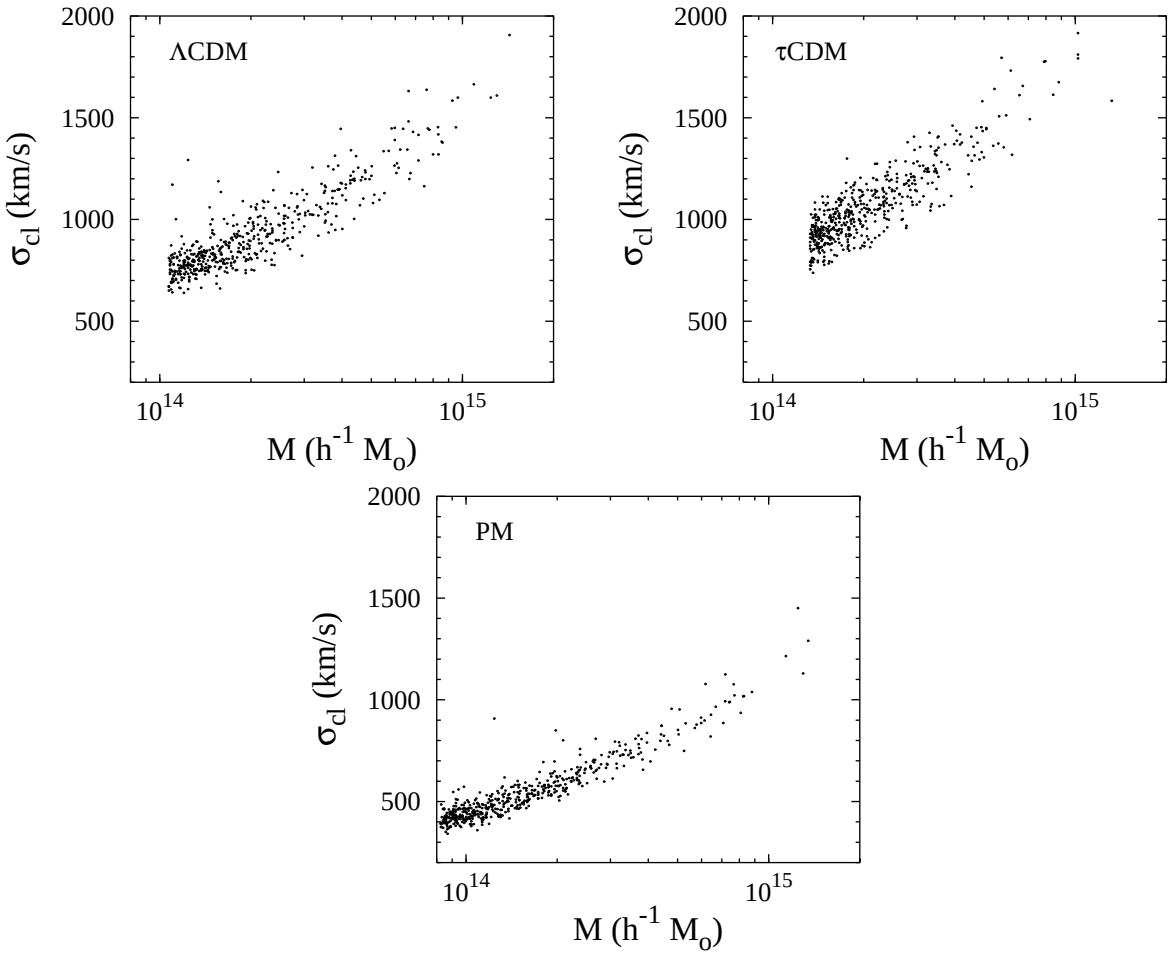

Figure 7. Intrinsic velocity dispersion of a cluster, σ_{cl} vs. the mass of the cluster, for the 509 most massive clusters . The clusters are defined using the FOF method with $b = 0.2$. The upper panel shows the velocity dispersions in the ΛCDM model, the middle panel in the τCDM model, and the lower panel in the PM model.

cluster is defined as

$$\sigma_{cl}^2 = \frac{1}{N_p} \sum_{i=1}^{N_p} |\vec{v}_i - \vec{v}_{cl}|^2. \quad (9)$$

The velocity dispersion determines the error for the mean velocity measurement for each individual cluster.

Fig. 7 shows the velocity dispersion of a cluster, σ_{cl}, versus the mass of the cluster. As expected, in the PM model the velocity dispersions inside clusters are smaller than in the AP^3M ΛCDM model. It is due to the small-scale smoothing inherent for the PM model. In this model, few clusters with a dispersion $\sigma_{cl} > 1000$ km s^{-1}, have the velocities $v_{cl} > 400$ km s^{-1}. In the ΛCDM model, high-velocity clusters with $v_{cl} > 800$ km s^{-1} ($M < 2 \times 10^{14} h^{-1} M_\odot$) have the dispersion $\sigma_{cl} < 1000$ km s^{-1}. In other words, all the clusters with $\sigma_{cl} > 1000$ km s^{-1}, have velocities $v_{cl} < 800$ km s^{-1}.

In this paper, we have studied peculiar velocities on scales that are close to the mean particle separation, λ_p, in the simulations. The PM code achieves the force resolution close to the separation λ_p, while the AP^{3}M code achives a force resolution smaller than λ_p. N-body simulations that use force resolution smaller than the mean particle separation are called "high-resolution" simulations. Are these high-resolution simulations really reliable on scales equal or below the mean separation length? Although several attempts have been made to answer this question (e.g. Efstathiou et al. 1985; 1988; Gelb & Bertchinger 1994; Suisalu & Saar 1995; Melott et al. 1997; Splinter et al. 1998; Hamana, Yoshida, Suto 2002), there is no clear answer yet. Our study shows that the rms peculiar velocity of massive clusters in an AP^{3}M simulation is smaller than in the similar PM simulation with the same mass resolution. The dependence of the rms peculiar velocity on the cluster mass in different simulations is different. Clearly, further work is needed (e.g. simulations with higher mass resolution) to solve this discrepancy between the AP^{3}M and PM simulations.

ACKNOWLEDGEMENTS

We thank J. Einasto, M. Einasto, P. Heinamäki, G. Hütsi and E. Saar for useful discussions. This work has been supported by the ESF grant 3601. The N-body simulations used in this paper are available at *http://www.mpa-garching.mpg.de/Virgo/virgoproject.html.* These simulations were carried out at the Computer Center of the Max-

Planck Society in Garching and at the EPCC in Edinburgh, as part of the Virgo Consortium project. The FOF programs used in this paper are available at *http://www-hpcc.astro.washington.edu*. These programs were developed in the University of Washington.

REFERENCES

Aghanim N., Gorski K.M., Puget J.L., 2001, A&A, 374, 1
Bahcall N.A., Gramann M., Cen R. 1994, ApJ, 436, 23
Bahcall N.A., Oh S.P. 1996, ApJ, 462, L49
Bardeen J.M., Bond J.R., Kaiser N., Szalay A.S. 1986, ApJ, 304, 15
Bond J.R., Efstathiou G., 1984, ApJ, 285, L45
Borgani S., da Costa L.N., Freudling W, Giovanelli R., Haynes M.P., Salzer, J., Wegner, G. 1997, ApJ, 482, L121
Borgani S., Bernardi M., da Costa L.N., Wegner G., Alonso M.V., Willmer C.N.A., Pellegrini P.S., Maia M.A.G., 2000, ApJ, 537, L1
Colless M., Saglia R.P., Burstein D., Davies R.L., McMahan R.K., Wegner G., 2001, MNRAS, 321, 277
Colberg J.M., White S.D.M., MacFarland T.J., Jenkins A., Pearce F.R., Frenk,C.S., Thomas P.A., Couchman H.M.P., 2000, MNRAS, 313, 229
Croft R.A.C., Efstathiou G., 1994, MNRAS, 268, L23
Couchman H.M.P., Thomas P.A., Pearce F.R., 1995, ApJ, 452, 797
Dale D.A., Giovanelli R., Haynes M.P., Campusano L,E., Hardy E. 1999, AJ, 118, 1489
Dalton, G.B., Croft, R.A.C., Efstathiou,G., Sutherland, W.J., Maddox, S.J., Davis, M. 1994, MNRAS, 271, L47
Efstathiou G., Davis M., Frenk C.S., White S.D.M., 1985, ApJS, 57, 241
Efstathiou G., Frenk C.S., White S.D.M., Davis M., 1988, MNRAS, 235, 715
Einasto, J., et al. 1997, Nature, 385, 139
Gelb J.M., Bertchinger E., 1994, ApJ, 436, 467
Giovanelli R., Haynes M.P., Herter T., Vogt N.P., Wegner G., Salzer J.J., da Costa L.N., Freudling W., 1997, AJ, 113, 22
Gramann M., 1988, MNRAS, 234, 569
Götz M, Huchra J.P., Brandenberger R.H., astro-ph:9811393
Hamana T, Yoshida N., Suto Y., astro-ph:0111158
Hockney R.W. & Eastwood J.W. 1981, Numerical simulations using particles (New York: McGraw-Hill)
Holzapfel W.L., Ade P.A.R., Church S.E., Mauskopf P.D., Rephaeli Y., Wilbanks T.M., Lange A.E., 1997, ApJ, 481, 35
Hudson M.J., Smith R.J., Lucey J.R., Schlegel D.J., Davies R.L., 1999, ApJ, 512, L79
Jenkins A. et al. (The Virgo Consortium), 1998, ApJ, 499, 20
Jenkins A., Frenk C.S., White S.D.M., Colberg J.M., Cole S., Evrard A.E., Couchman H.M.P., Yoshida N., 2001, MNRAS, 321, 372
Lamarre J.M. et al., 1998, ApJ, 507, L5
Lauer T.R., Postman M. 1994, ApJ, 425, 418
Melott A.L., Splinter R.J., Shandarin S.F., Suto Y., 1997, ApJ, 479, L79
Moscardini L., Branchini E., Brunozzi P.T., Borgani S., Plionis M., Coles P. 1996, MNRAS, 282, 384
Pearce F.R., Couchman H.M.P., 1997, NewA, 2, 411
Rephaeli Y., Lahav O. 1991, ApJ, 372, 21
Sheth R.K., Diaferio A., 2001, MNRAS, 322, 901
Splinter R.J., Melott A.L., Shandarin S.F., Suto Y., 1998, ApJ, 497, 38
Suhhonenko I., Gramann M., 1999, MNRAS, 303, 77
Suisalu I., Saar E., 1995, astro-ph: 9511120
Sunyaev R.A., Zel'dovich Y.B., 1980, MNRAS, 190, 413
Watkins R. 1997, MNRAS, 292, L59
Willick J.A., Courteau S., Faber S.M., Burstein D., Dekel A., Strauss M.A., 1997, ApJS, 109, 333

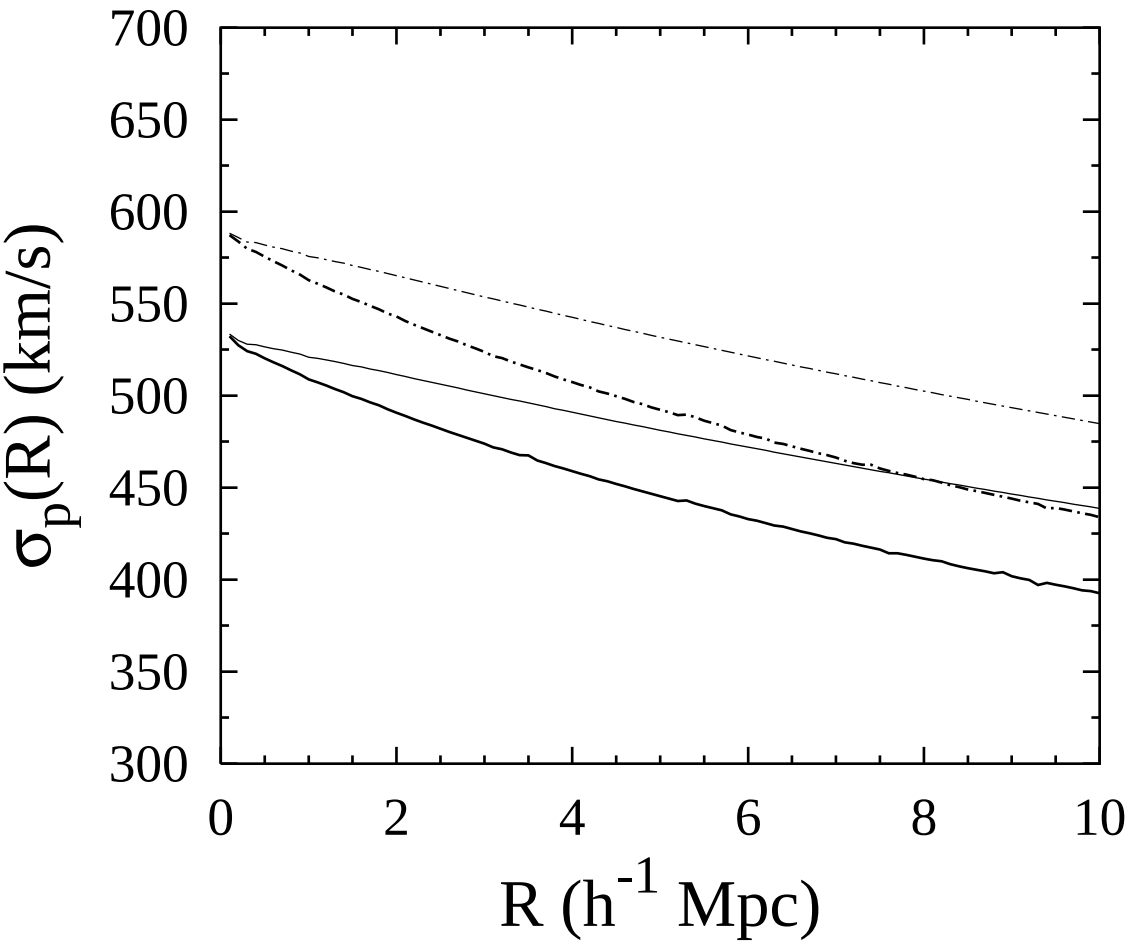
700
650
600
550
500
450
400
350
300
0
2
4
6
8
10
σp(R) (km/s)
R (h-1 Mpc)

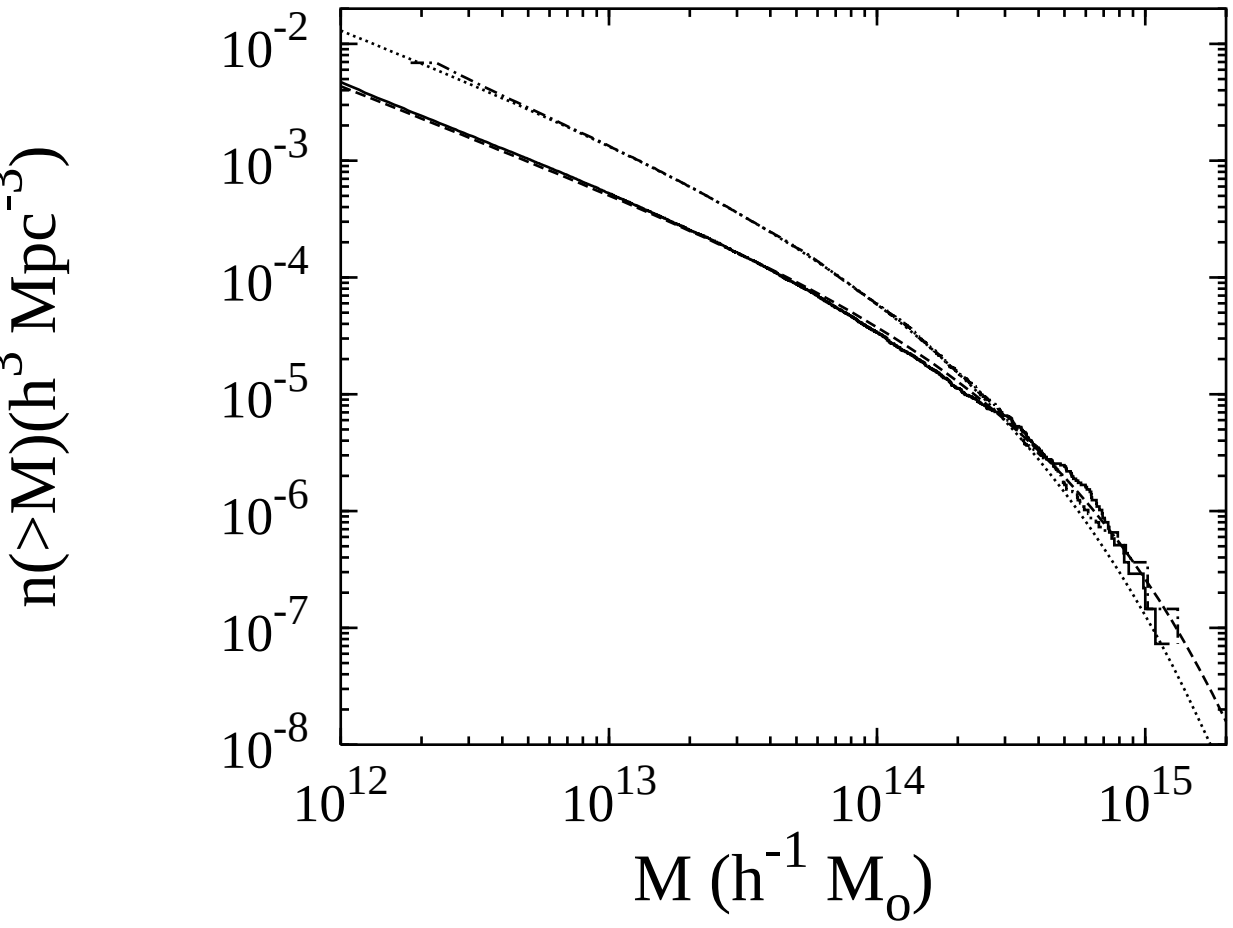
10^{-2}
10^{-3}
10^{-4}
10^{-5}
10^{-6}
10^{-7}
10^{-8}
10^{12}
10^{13}
10^{14}
10^{15}
n(>M)(h^3 Mpc^{-3})
M (h^{-1} M$_o$)

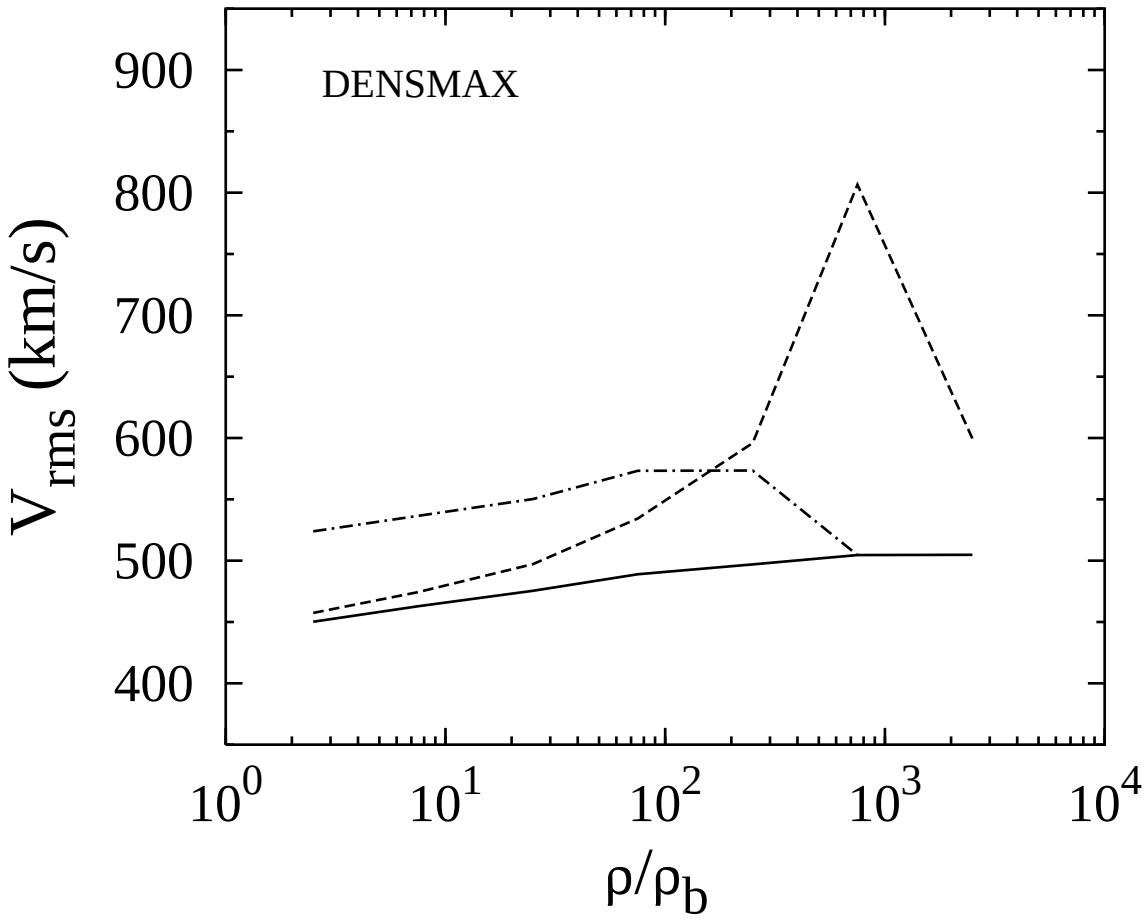
DENSMAX
900
800
700
600
500
400
V_{rms} (km/s)
10^0
10^1
10^2
10^3
10^4
ρ/ρ_b

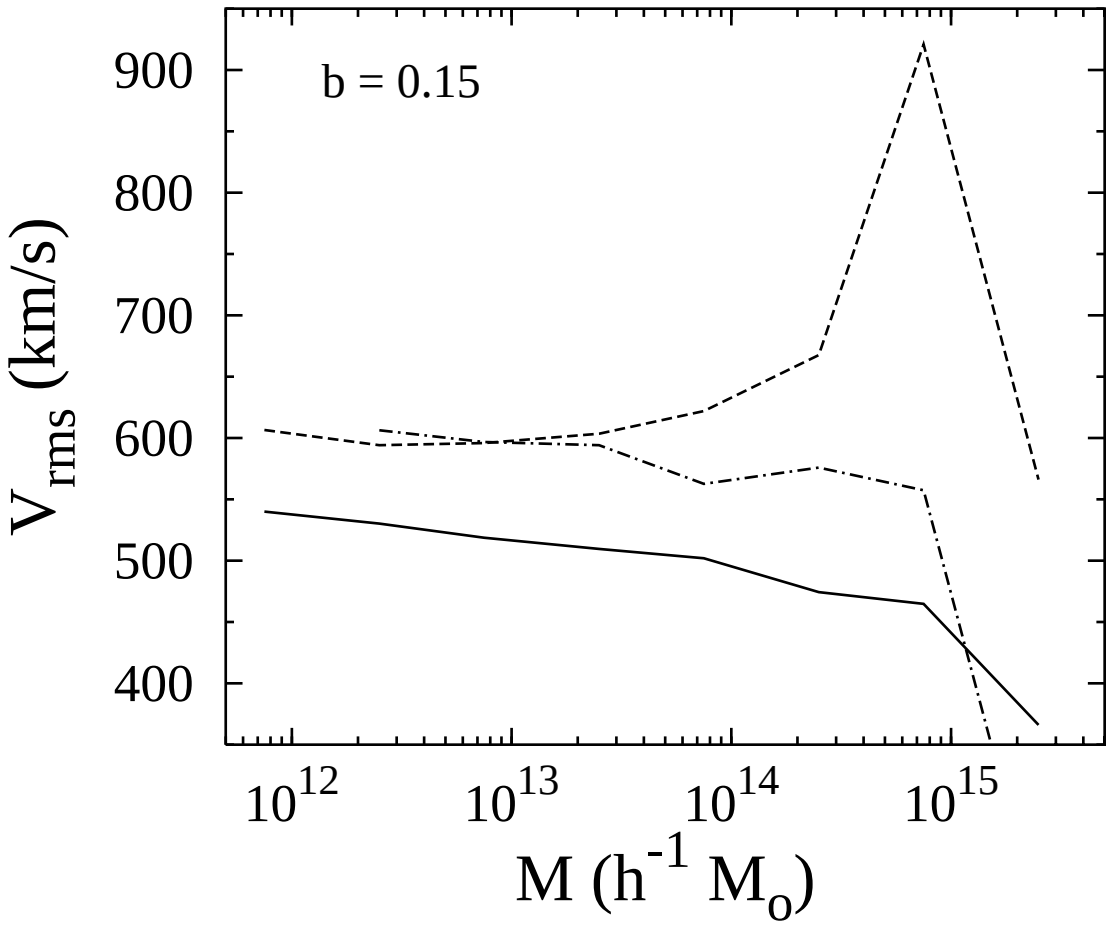
b = 0.15
900
800
700
600
500
400
V_{rms} (km/s)
10^{12}
10^{13}
10^{14}
10^{15}
M (h^{-1} M_o)

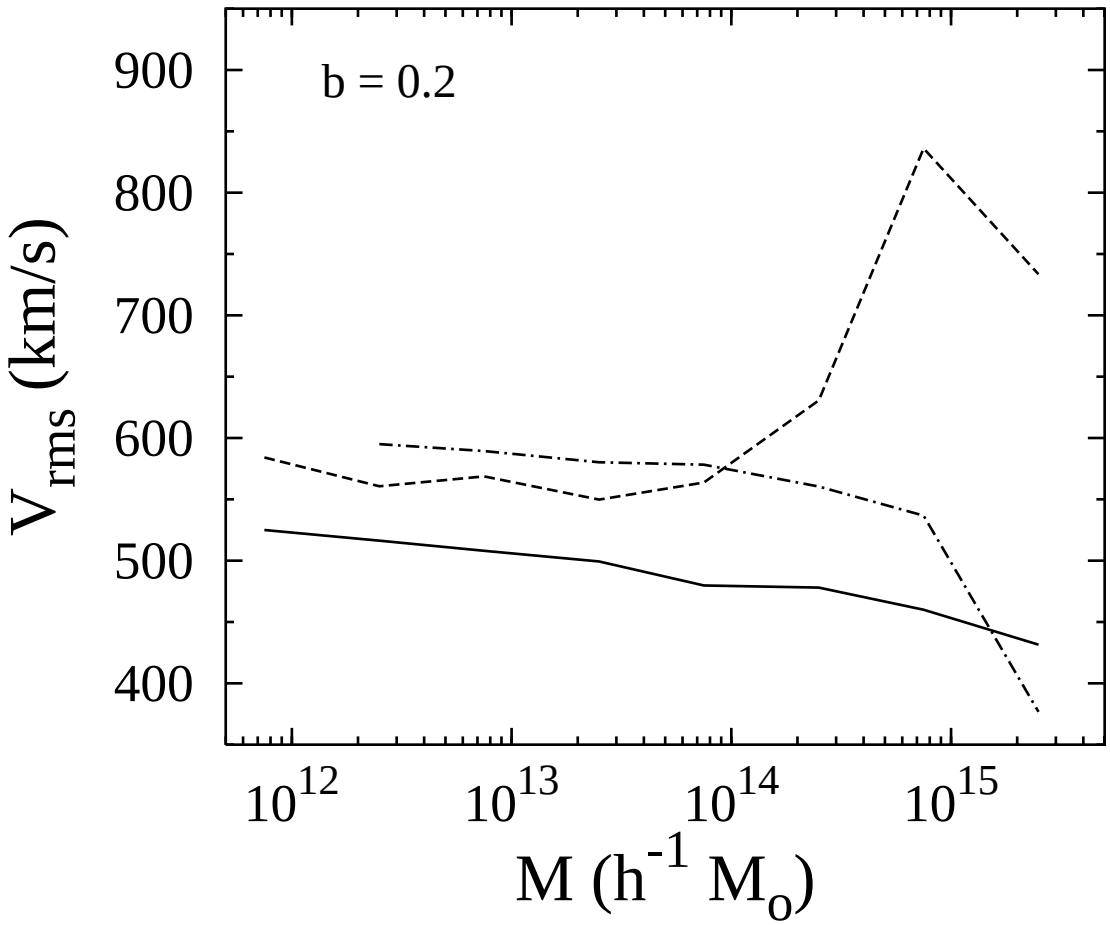
b = 0.2
900
800
700
600
500
400
V_{rms} (km/s)
10^{12}
10^{13}
10^{14}
10^{15}
M (h^{-1} M_o)

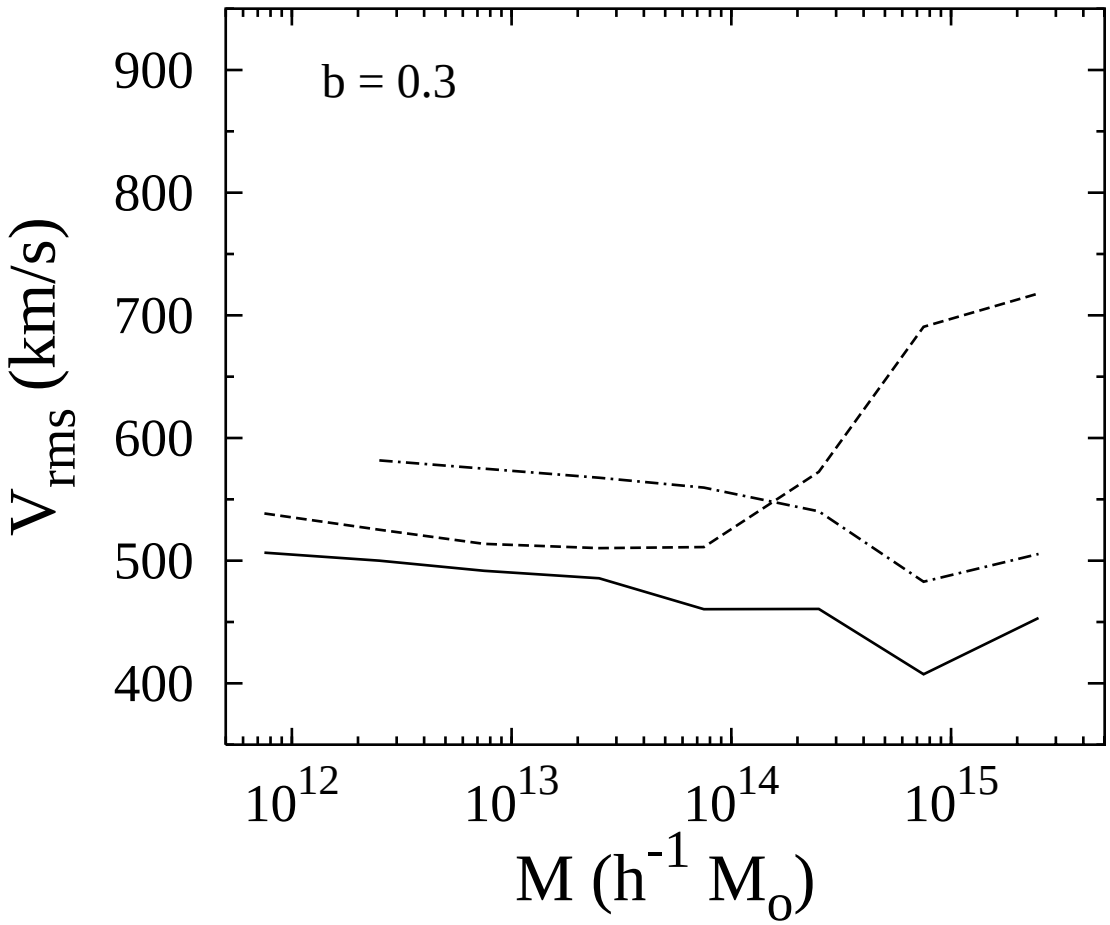
b = 0.3
900
800
700
600
500
400
V_{rms} (km/s)
10^{12}
10^{13}
10^{14}
10^{15}
M (h^{-1} M_o)

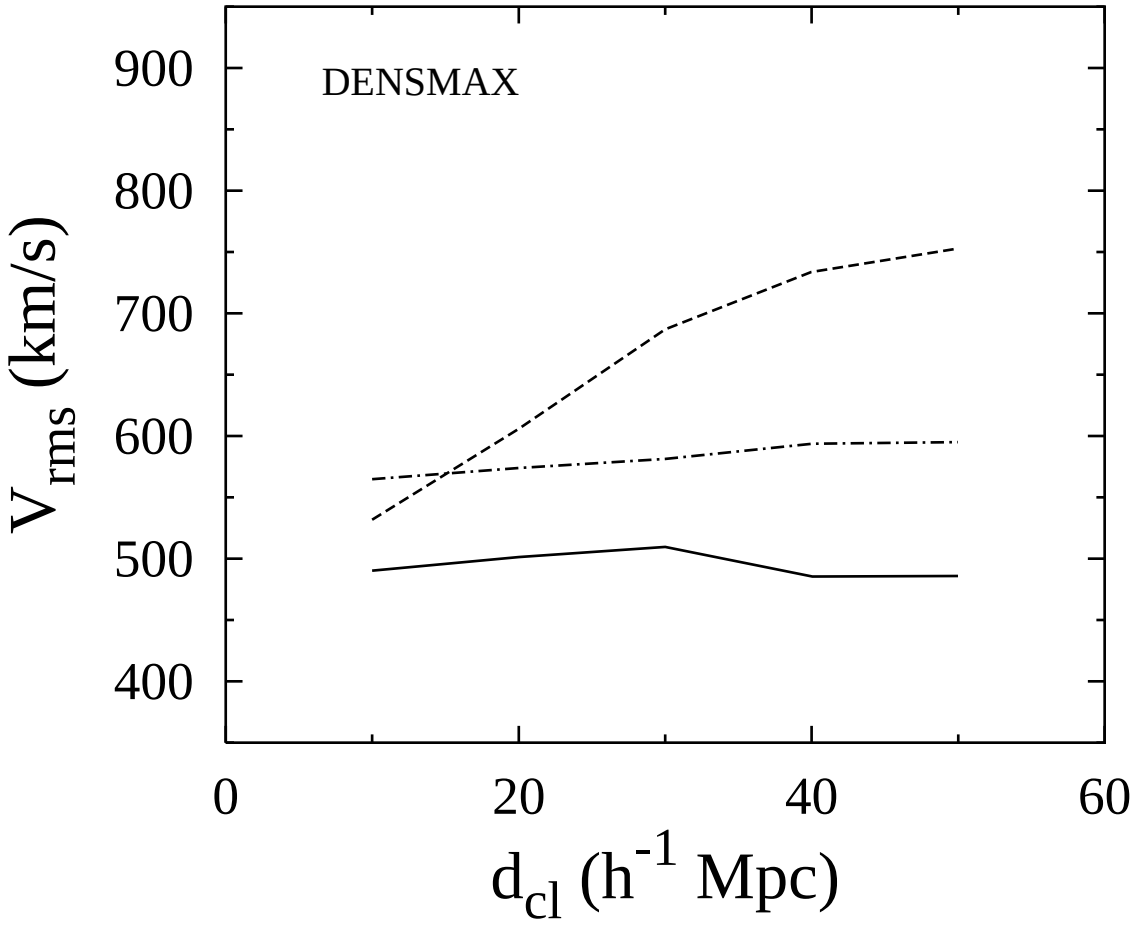
DENSMAX
900
800
700
600
500
400
0
20
40
60
V_{rms} (km/s)
d_{cl} (h^{-1} Mpc)

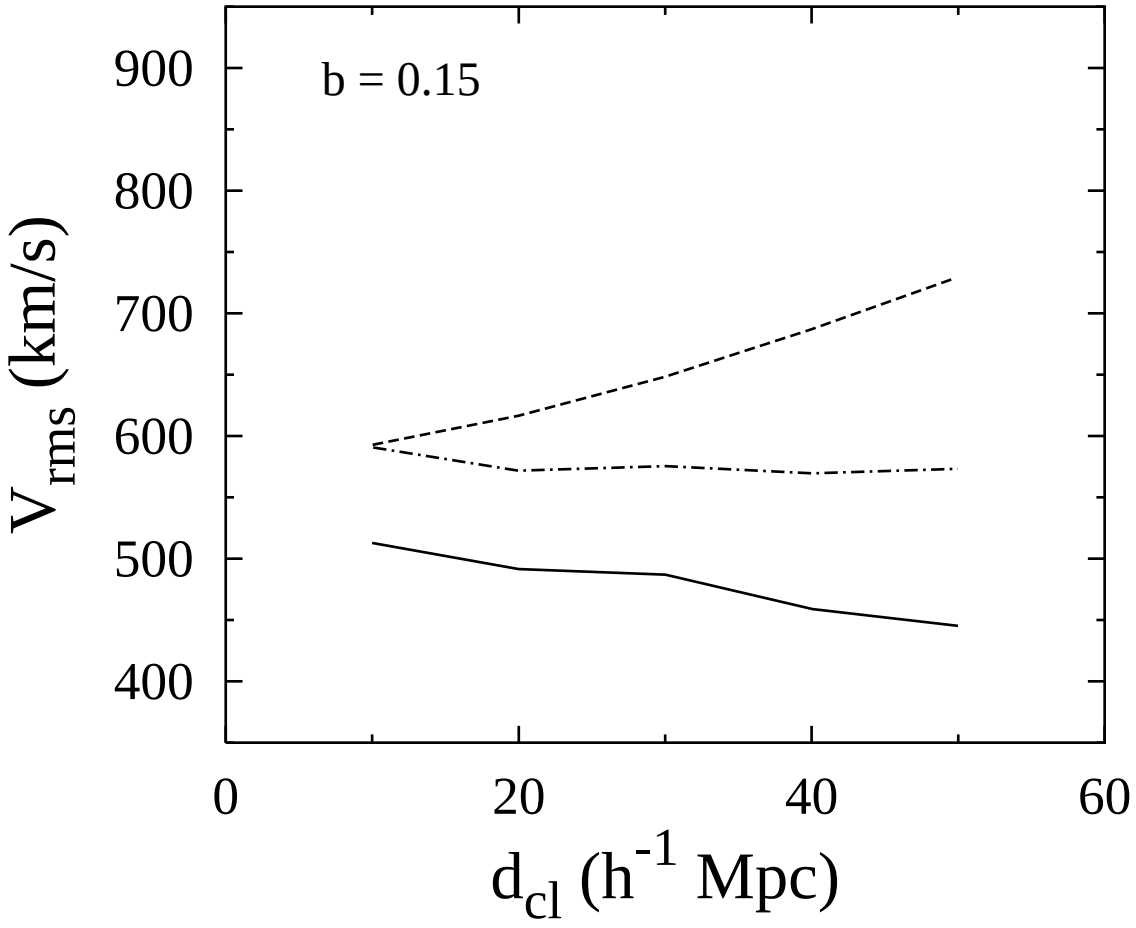
b = 0.15
900
800
700
600
500
400
0
20
40
60
V_{rms} (km/s)
d_{cl} (h^{-1} Mpc)

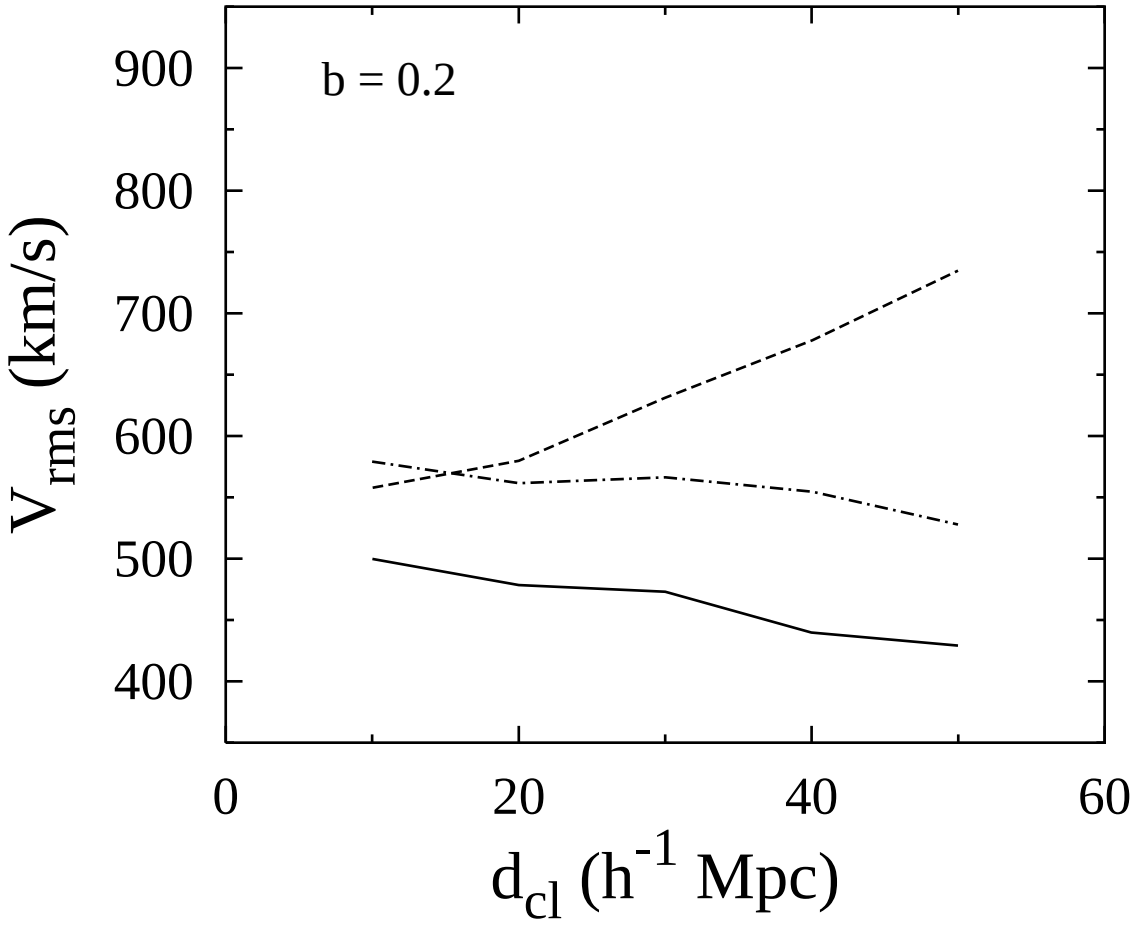
b = 0.2
900
800
700
600
500
400
0
20
40
60
V_{rms} (km/s)
d_{cl} (h^{-1} Mpc)

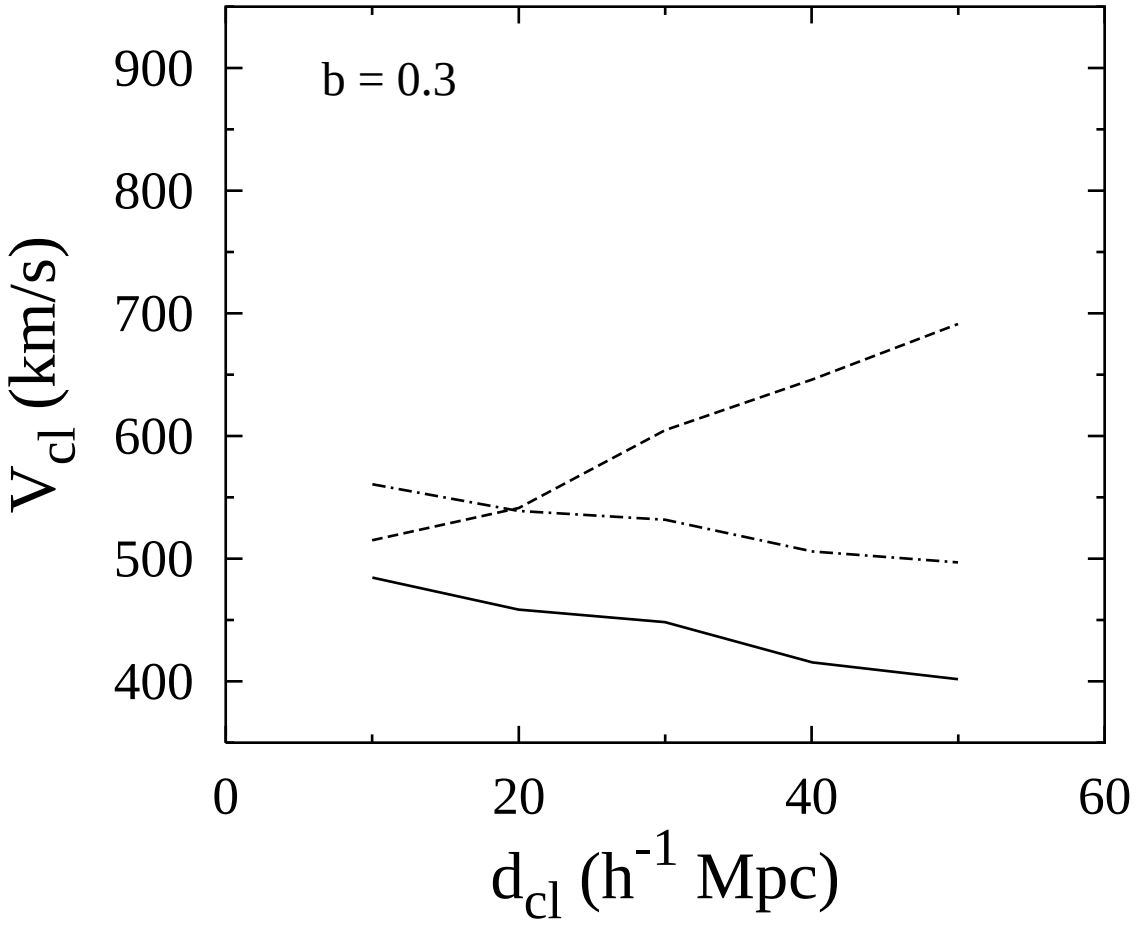
b = 0.3
900
800
700
600
500
400
V_{cl} (km/s)
0
20
40
60
d_{cl} (h^{-1} Mpc)

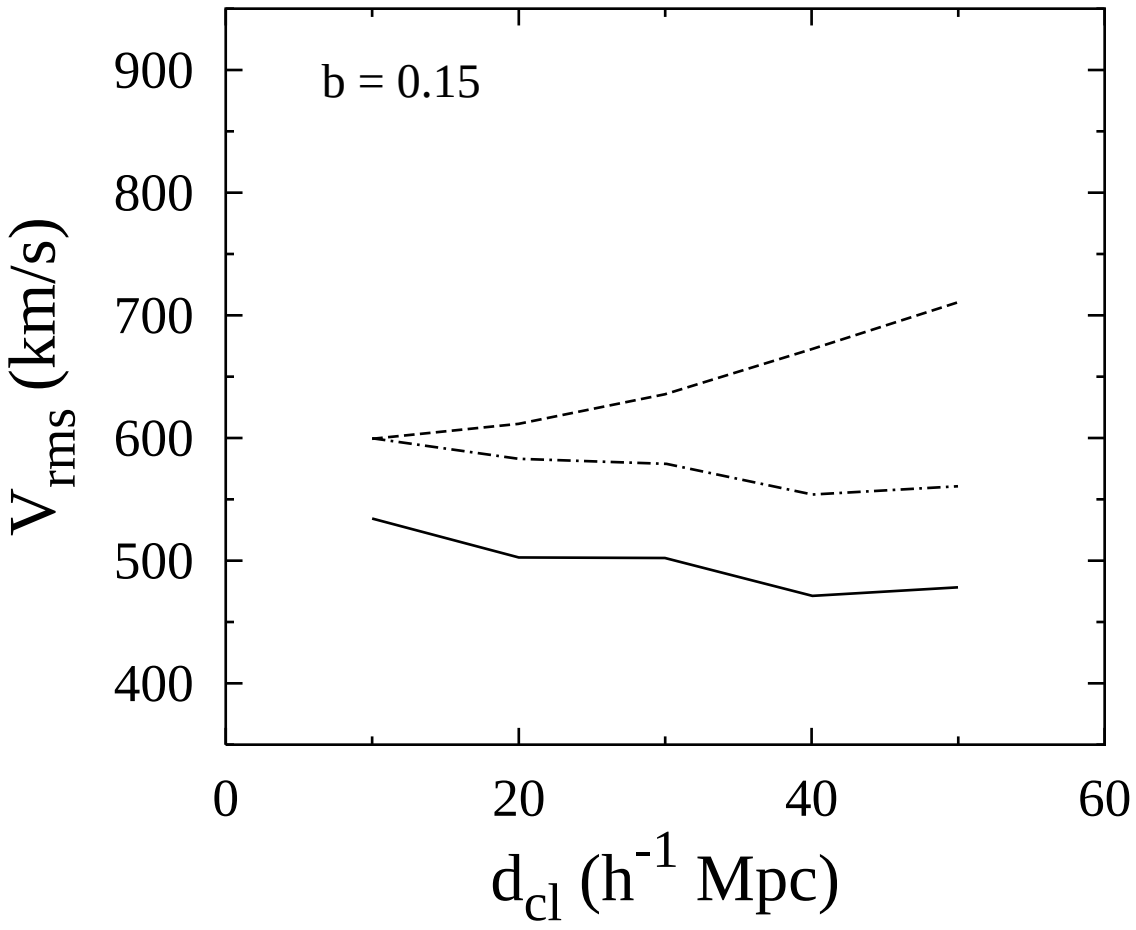
b = 0.15
900
800
700
600
500
400
0
20
40
60
V_{rms} (km/s)
d_{cl} (h^{-1} Mpc)

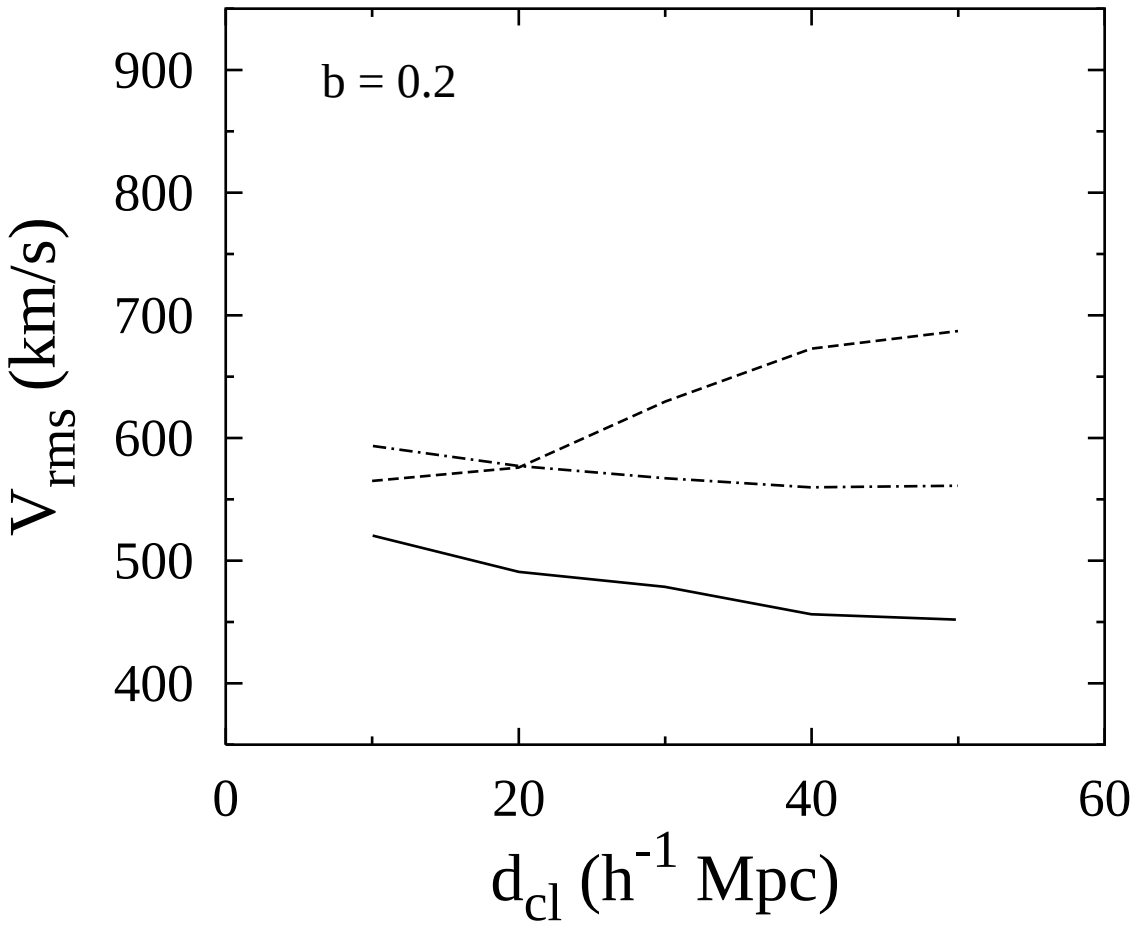
b = 0.2
900
800
700
600
500
400
0
20
40
60
V_{rms} (km/s)
d_{cl} (h^{-1} Mpc)

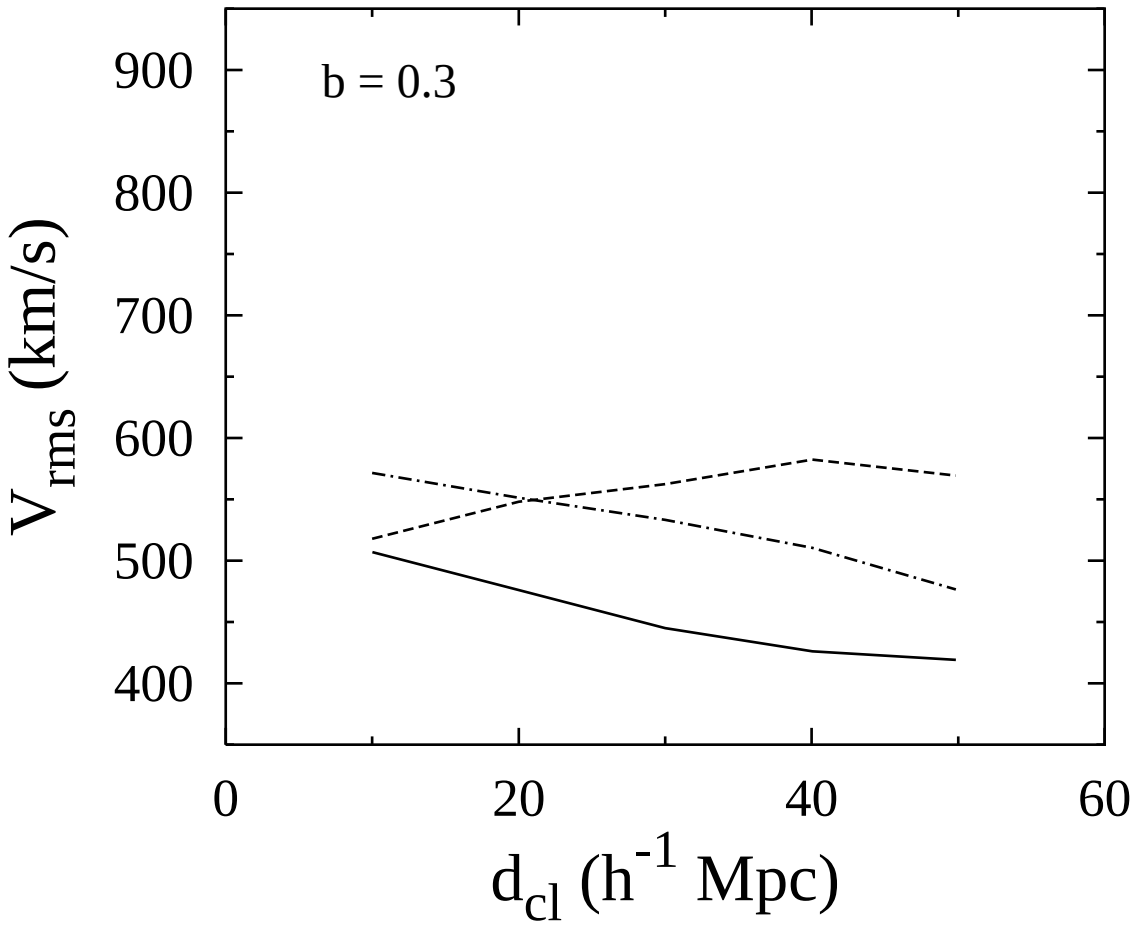
b = 0.3
900
800
700
600
500
400
V_{rms} (km/s)
0
20
40
60
d_{cl} (h^{-1} Mpc)

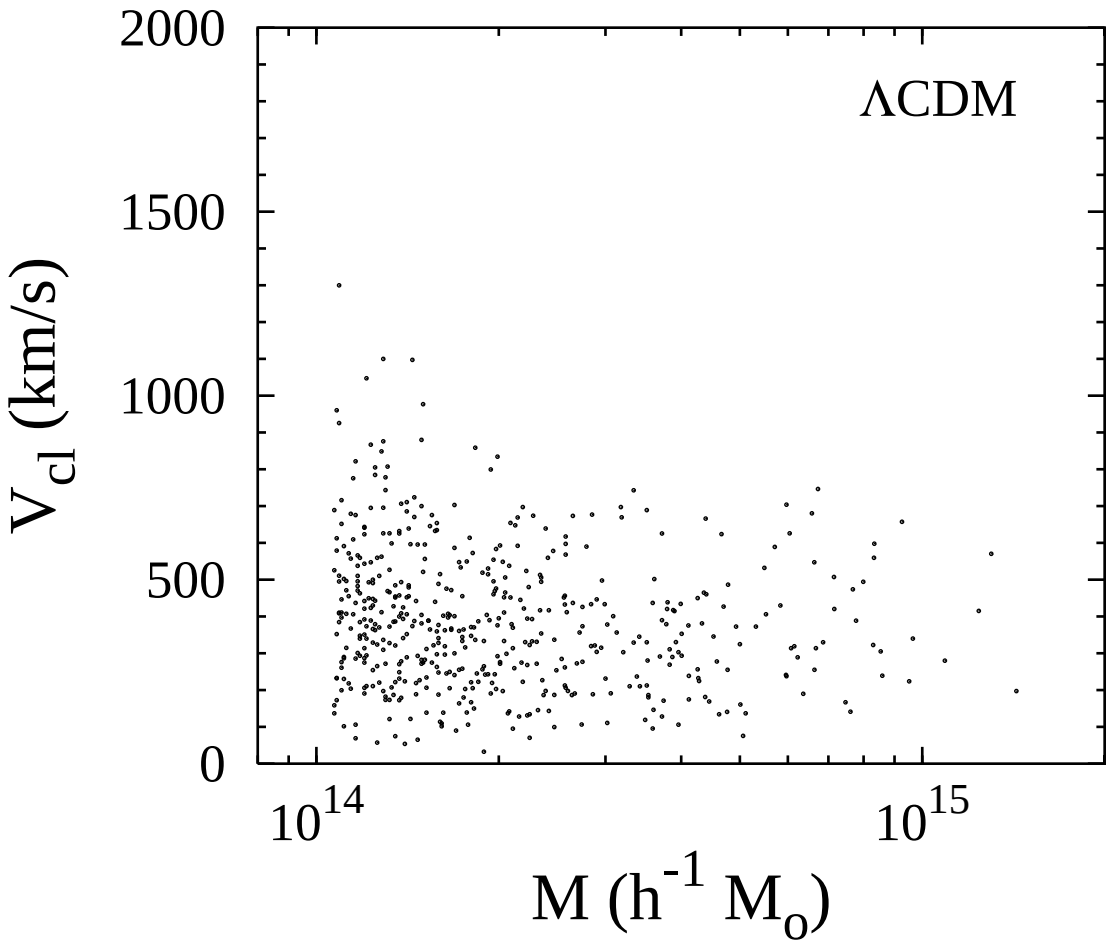
2000
1500
1000
500
0
ΛCDM
V_{cl} (km/s)
10^{14}
10^{15}
M (h^{-1} M_o)

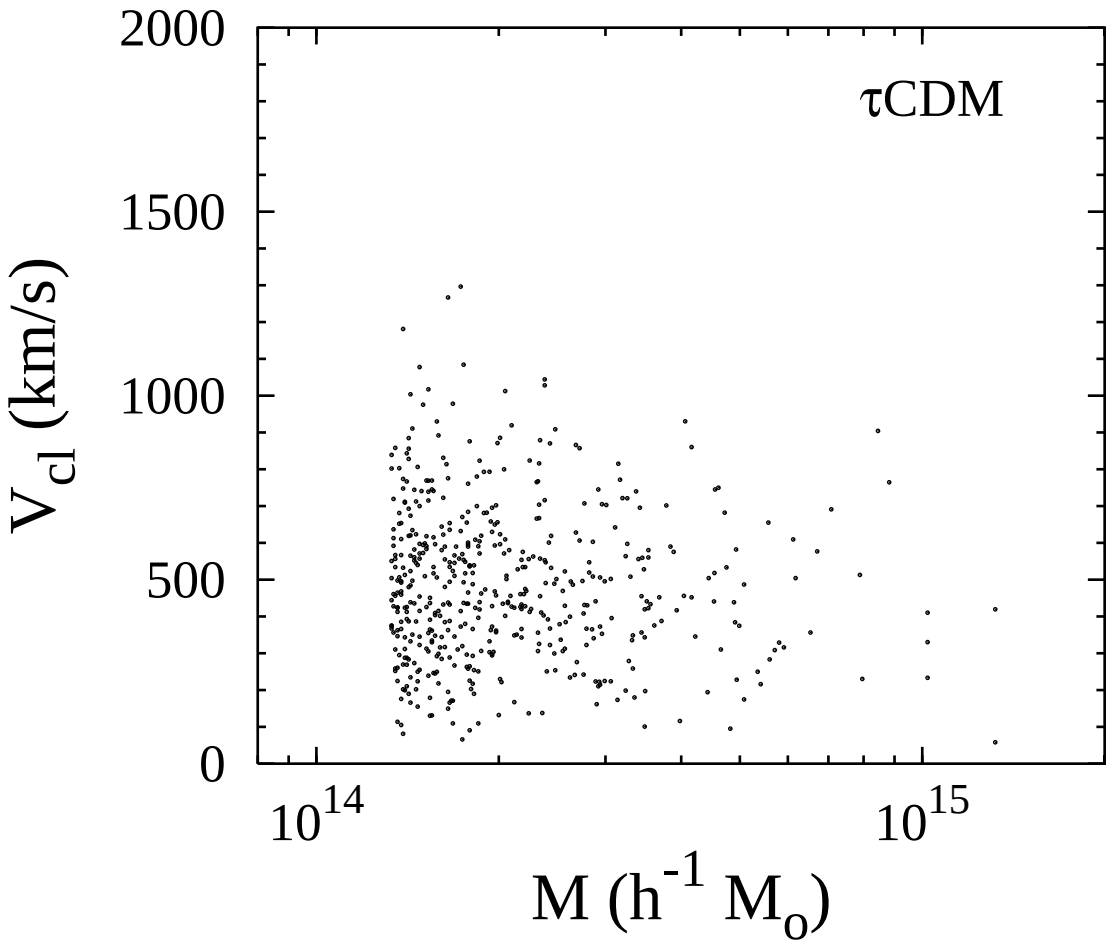
2000
1500
1000
500
0
τCDM
V_{cl} (km/s)
10^{14}
10^{15}
M (h^{-1} M_o)

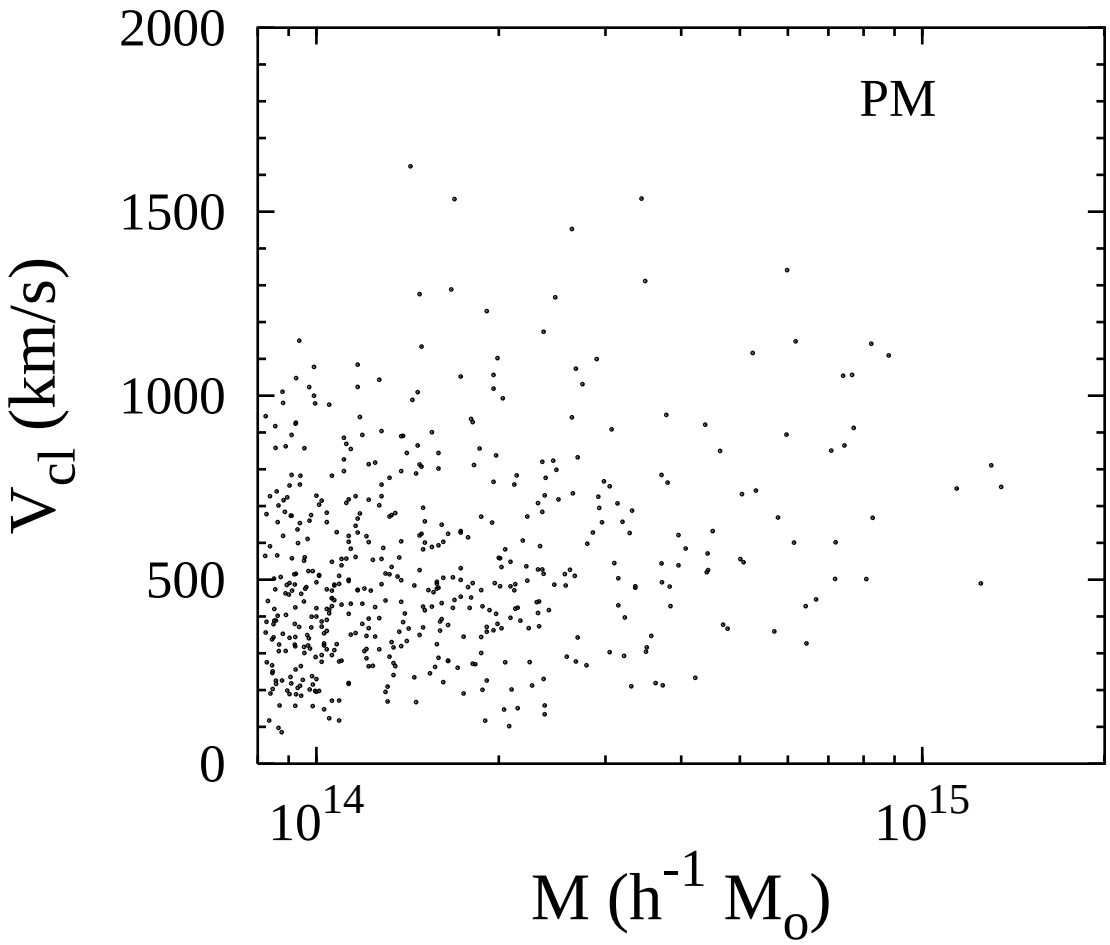
2000
1500
1000
500
0
PM
V_{cl} (km/s)
10^{14}
10^{15}
M (h^{-1} M_o)

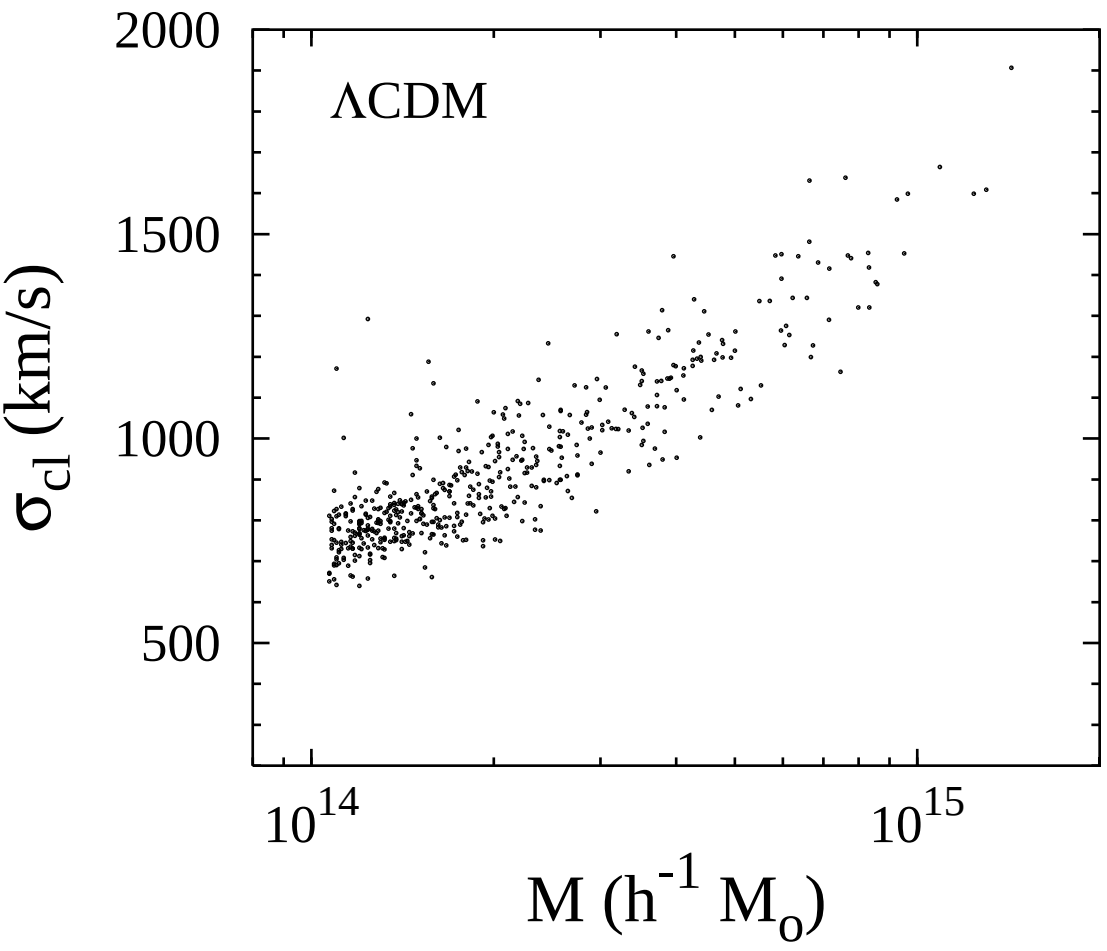
ΛCDM
2000
1500
1000
500
σ_{cl} (km/s)
10^{14}
10^{15}
M (h^{-1} M_o)

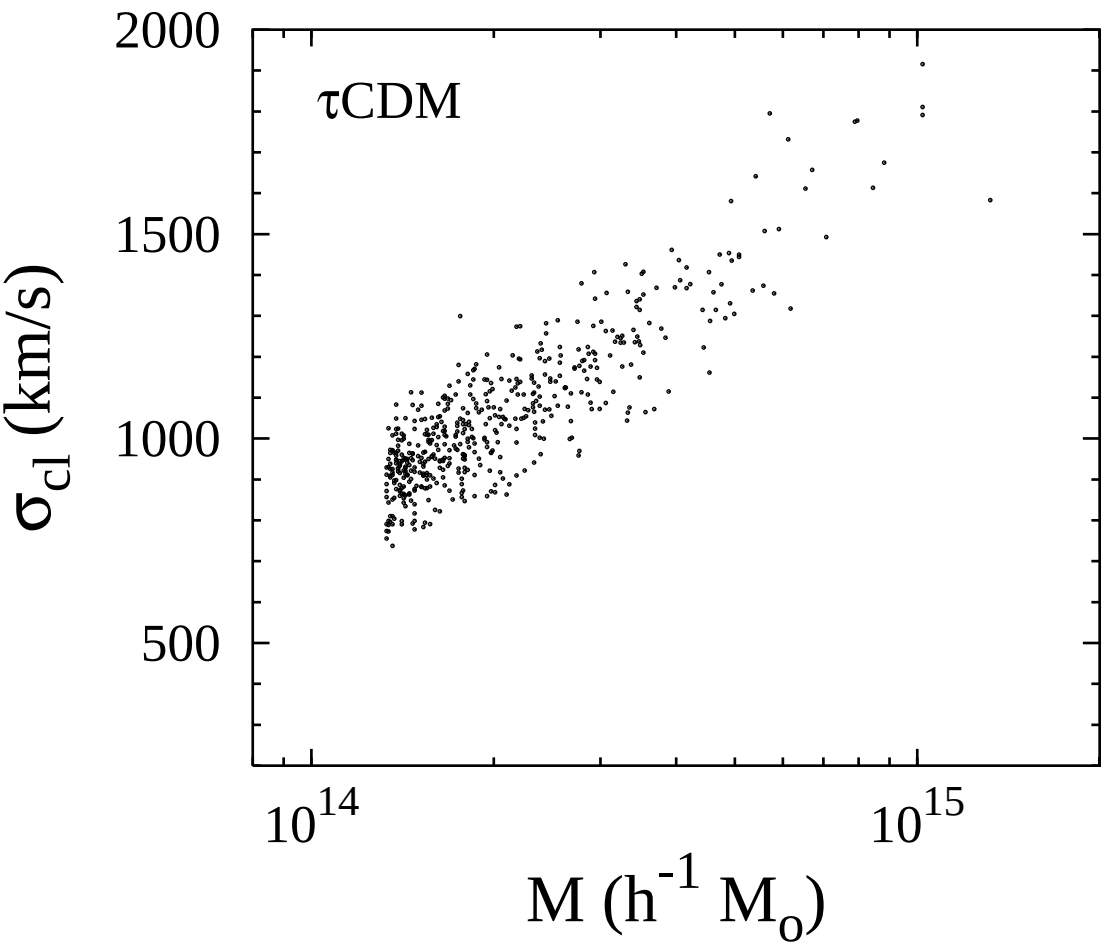
τCDM
2000
1500
1000
500
σ_{cl} (km/s)
10^{14}
10^{15}
M (h^{-1} M_o)

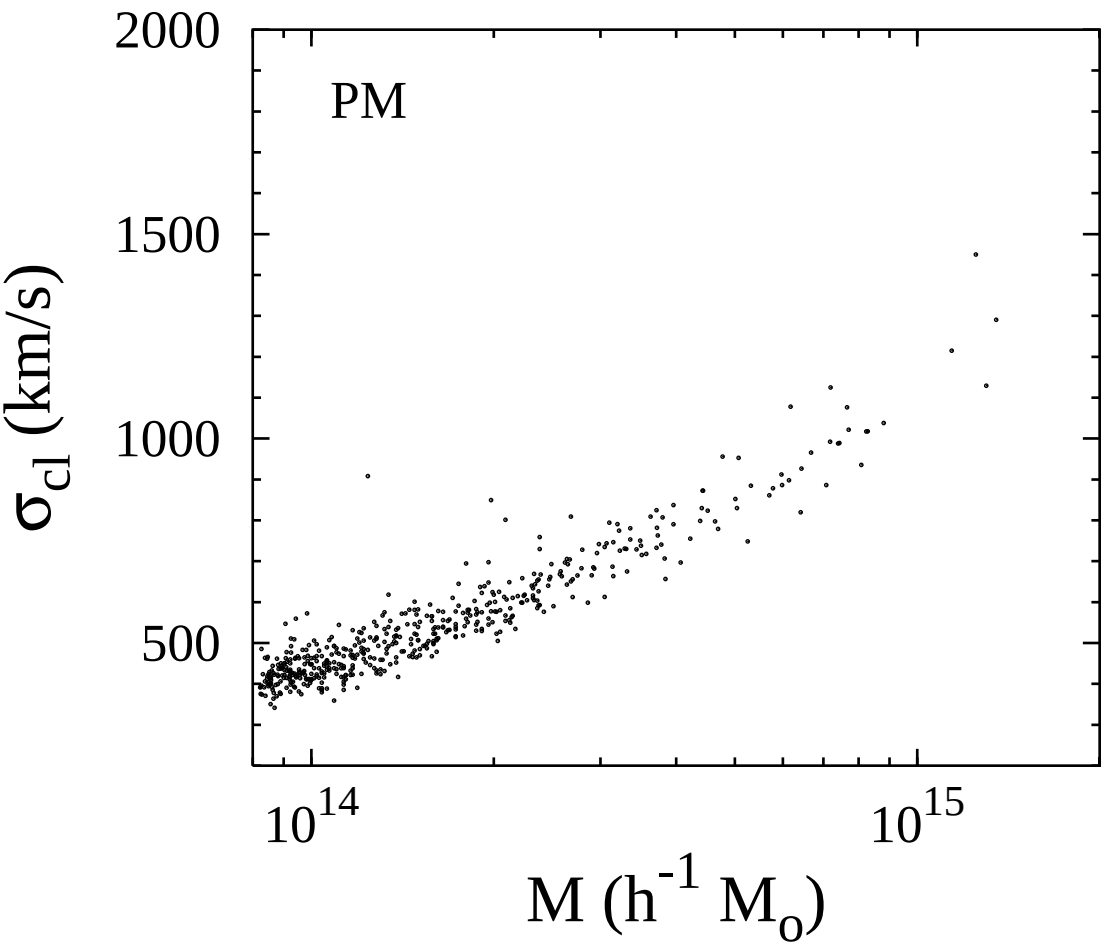
PM
2000
1500
1000
500
σ_{cl} (km/s)
10^{14}
10^{15}
M (h^{-1} M_o)